

# PRELIMINARY DRAFT: USER MANUAL

## FOR

# TREERING 2000

**Harold C. Fritts<sup>1\*</sup>, Alex V. Shashkin<sup>2</sup>, Debbie L. Hemming<sup>1,3</sup>,  
Steven W. Leavitt<sup>1</sup>, William Edward Wright<sup>1</sup>, Geoffery M.  
Downs<sup>4</sup>**

1. Laboratory of Tree Ring Research, Building #58, University of Arizona, Tucson. Arizona. 85719. U.S.A.
2. Department of Forest, Akdemgorodok, Krasnoyarsk, 660036, Russia.
3. ESER, Weizmann Institute of Science. Rehovot. 76100. Israel.
4. CSIRO-GPO Box 252-12, Hobart, Australia.

\* Corresponding Author

<b><u>I. MODEL DESCRIPTION</u></b> .....	<b>2</b>
<u>I.1. INTRODUCTION</u> .....	2
<u>I.2. PHOTOSYNTHESIS</u> .....	2
<u>I.3. TRANSPIRATION</u> .....	4
<u>I.4. UTILIZATION OF PHOTOSYNTHATES</u> .....	5
<u>I.4.i. Maintenance Respiration</u> .....	5
<u>I.4.ii. Growth</u> .....	5
<u>I.5. WATER ABSORPTION BY ROOTS</u> .....	6
<u>I.6. GROWTH</u> .....	7
<u>I.6.i. Leaves</u> .....	7
<u>I.6.ii. Stem</u> .....	7
<u>I.6.ii.a. Division of cambium cells</u> .....	8
<u>I.6.ii.b. Cell enlargement</u> .....	10
<u>I.6.ii.c. Cell maturation</u> .....	0
<u>I.6.iii. Roots</u> .....	12
<u>I.7. ALLOCATION, REDISTRIBUTION AND STORAGE OF SUBSTRATE</u> .....	13
<u>I.8. SOIL WATER</u> .....	14
<u>I.9. ISOTOPE CALCULATIONS</u> .....	15
<u>I.9.i. Carbon</u> .....	15
<u>I.9.i.a. Photosynthate</u> .....	15
<u>I.9.ii Oxygen and Hydrogen</u> .....	16
<u>I.9.ii.a. Soil Water / Xylem Water</u> .....	16
<u>I.9.ii.b. Leaf Water Model</u> .....	17
<u>I.9.ii.c. Photosynthate and cellulose</u> .....	18
<b><u>EXTERNAL INPUTS</u></b> .....	<b>18</b>
<u>II.1. DAILY METEOROLOGICAL DATA</u> .....	18
<u>II.1.i. Maximum Temperature</u> .....	19
<u>II.1.ii. Minimum Temperature</u> .....	20
<u>II.1.iii. Precipitation</u> .....	21
<u>II.1.iv. Dew Point Temperature</u> .....	23
<u>II.2. ISOTOPE INPUTS</u> .....	24
<u>II.2.i. <math>d^{13}C</math> of atmospheric <math>CO_2</math></u> .....	24
<u>II.2.ii. <math>d^{18}O</math> and <math>dD</math> of precipitation and atmospheric water vapor</u> .....	24

<a href="#">II.3. ALLOMETRIC DATA</a> .....	26
<a href="#">II.3.i. Tree age:height:radius curve</a> .....	26
<a href="#">II.3.ii. Relationship between volume and mass of sapwood and the volume of live cells in the sapwood</a> .....	30
<a href="#">II.4. PARAMETERS</a> .....	32
<a href="#">III. REFERENCES</a> .....	47

## I. MODEL DESCRIPTION

### I.1. Introduction

The most recent published version of the model, called TreeRing, is included in Fritts *et al.* (1999). It is basically a physiological model describing details of tree growth and cell structure along a single radius of a conifer stem as a function of daily maximum and minimum temperature and precipitation. Refinements now include daily dew point observations, annual atmospheric CO<sub>2</sub> concentration ([CO<sub>2</sub>]) and δ<sup>13</sup>C composition, and the δ<sup>18</sup>O and δD of precipitation and atmospheric water vapor. A large number of input parameters control the constants of the equations, the range of variation, and limitations to the various processes governing the growth of the tree. Additional input parameters define annual stem, leaf and root growth. These values are obtained from measurements of the age/height relationships of the simulated forest stand.

A summary output describes annual ring characteristics including ring width, cell number, cell size variation and cell-wall thickness within the simulated annual ring. These four ring characteristics along with a calculated ring width index are statistically compared to measurements of ring width, cell numbers, cell size, and wall thickness along dendrochronologically dated cores extracted from the modeled tree. A ring-width index of the modeled trees is calculated from a replicated chronology sampled from the same site. The degree of correlation and the coefficients of regression for these comparisons provide automatic validation as to how well the simulations mimic the actual ring characteristics of the tree.

Additional summaries include isotopic concentrations in each cell along with daily outputs of a large number of model inputs and outputs. A separate graphics program is developed to plot the annual ring characteristics, estimated by the model and measured from the cores, along with daily estimates or measurements of 12 variables selected from more than 78 different outputs from the model. This provides a highly flexible means of evaluating all aspects of the model calculations.

Details of the modeled processes are summarized in the following sections.

### I.2. Photosynthesis

The rate of photosynthesis ( $p$ ) is described in the model by the following system of equations:

$$(2.1) \quad p = \frac{C_a - C_i}{R^c}$$

$$p = P_{\max} f_c(C_i) f_T(T) f_I(I)$$

where,  $C_a$  is concentration of  $\text{CO}_2$  in the air [ $\text{mM m}^{-3}$ ],  $C_i$  is concentration of  $\text{CO}_2$  inside in the leaf [ $\text{mM m}^{-3}$ ],  $R^c$  is the resistance of leaves to diffusion  $\text{CO}_2$  [ $\text{s m}^{-1}$ ],  $P$  is the photosynthetic rate [ $\text{mM CO}_2 \text{ m}^{-2} \text{ s}^{-1}$ ],  $f_c$ ,  $f_T$  and  $f_I$  are normalized functions of dependence of photosynthesis on  $C_i$ , temperature  $T$ , incoming irradiation  $I$  and maximum rate of photosynthesis  $P_{max}$ .

The dependence of photosynthesis on  $C_i$  is:

$$(2.2) \quad \begin{aligned} f_c(C_i) &= 0, & \text{when } C_i < a \\ f_c(C_i) &= (C_i - a)/(b - a), & \text{when } a < C_i < b \\ f_c(C_i) &= 1, & \text{when } C_i > b \end{aligned}$$

where,  $a$  and  $b$  are minimum and maximum  $C_i$  respectively.

With an average light flux, the function for  $I$  ( $[\text{J m}^{-2} \text{ s}^{-1}]$  corresponding to photosynthetically active radiation),  $f_I$ , is a Michaelis-Menton type curve:

$$(2.3) \quad f_I = I/(I + I^*)$$

where,  $I^*$  is the Michaelis-Menton constant for radiation at which photosynthesis reaches half maximum. The temperature dependency of photosynthesis is:

$$(2.4) \quad \begin{aligned} f_T &= 0, & \text{when } T < T_{min} \\ f_T &= (T - T_{min})/(T_1 - T_{min}), & \text{when } T_{min} \leq T \leq T_1 \\ f_T &= 1, & \text{when } T_1 \leq T \leq T_2 \\ f_T &= (T_{max} - T)/(T_{max} - T_2), & \text{when } T_2 \leq T \leq T_{max} \end{aligned}$$

where,  $T_{min}$ ,  $T_1$ ,  $T_2$ , and  $T_{max}$  are the minimum, optimal, maximum optimal and maximum temperatures respectively.

From equations 2.1 and 2.2 the rate of photosynthesis is:

$$(2.5) \quad \begin{aligned} p &= P_m(T, I) \frac{C_a - a}{b - a + P_m(T, I)R^c}, & P_m R^c \geq C_a - b \\ p &= P_m, & P_m R^c \leq C_a - b \end{aligned}$$

where,  $P_m$  is the maximum photosynthesis,  $P_{max}$ .

For conditions when  $\text{CO}_2$  inside of the leaf is not limiting the rate of photosynthesis leaf resistance increases according to the following equation:

$$(2.6) \quad R_p^c = \frac{C_a - b}{P_m}$$

where,  $R_p^c$  is the leaf resistance to diffusion of  $\text{CO}_2$  at the specific photosynthetic rate,  $p$ . In this case the  $b = C_i$  if  $R_p^c$  is less than maximum resistance  $R_{max}^c$  and  $C_i = C_a - P_m R_{max}^c$ ,  $R_p^c = R_{max}^c$  if  $R_p^c$  is more than  $R_{max}^c$ .

Photosynthesis for the entire crown ( $P$ ) is estimated using:

$$(2.7) \quad P = p \times D \times \mathbf{s} \times M_l$$

where,  $D$  is the day length [s],  $\mathbf{s}$  is the coefficient for transforming foliage mass into surface area [ $\text{m}^2 \text{kg}^{-1}$ ] and  $M_l$  is the mass of foliage [kg].

### I.3. Transpiration

The potential transpiration by leaves is given by:

$$(3.1) \quad tr^p = \frac{\Delta \mathbf{r}}{R_{min}^w}$$

where,  $tr^p$  is potential transpiration [ $\text{kg H}_2\text{O m}^{-2} \text{s}^{-1}$ ],  $\Delta \mathbf{r}$  is the water vapor density deficit [ $\text{kg m}^{-3}$ ],  $R_{min}^w$  is the minimum resistance of leaves to water diffusion [ $\text{m s}^{-1}$ ].

The water vapour density deficit is determined from equation 3.2:

$$(3.2) \quad \Delta \mathbf{r} = \tilde{n}_a \times 0.622 \times \frac{e_s - e}{P_{atm}}$$

where,  $\mathbf{r}_a$  is air density [ $\text{kg m}^{-3}$ ],  $P_{atm}$  is the atmospheric pressure [mbar],  $e$  is the water vapor pressure at a particular temperature, and  $e_s$  is the saturated water vapor pressure at the same temperature.  $e$  and  $e_s$  are estimated as follows:

$$(3.3) \quad \begin{aligned} e(T) &= \exp\left(1.80985 + \frac{17.27 \times T_d}{237.3 + T_d}\right), T \geq 0.0 \\ e(T) &= \exp\left(1.80985 + \frac{21.87 \times T_d}{265.5 + T_d}\right), T < 0.0 \\ e_s(T) &= \exp\left(1.80985 + \frac{17.27 \times T}{237.3 + T}\right), T \geq 0.0 \\ e_s(T) &= \exp\left(1.80985 + \frac{21.87 \times T}{265.5 + T}\right), T < 0.0 \end{aligned}$$

where,  $T_d$  is the dew point temperature at the particular dry bulb air temperature,  $T$ .

The total potential transpiration from the crown ( $Tr^p$ ) is estimated using the equation:

$$(3.4) \quad Tr^P = tr^P \times D \times \mathbf{s} \times M_1$$

where, the coefficients  $D$ ,  $\mathbf{s}$  and  $M_1$  are the same as in equation 2.7.

## I.4. Utilization of photosynthates

### I.4.i. Maintenance Respiration

Maintenance respiration is dependent upon temperature and substrate availability:

$$(4.1) \quad Rm_i = \hat{a}_{0i} \frac{s_i}{s_i + s_i^*} e^{\hat{a}_{i,T}} M_i \quad \text{where } i = l, s, r$$

where,  $Rm_i$  is the rate of maintenance respiration [mM CO<sub>2</sub> d<sup>-1</sup>],  $\hat{a}_{0i}$  is the substrate uptake for maintenance respiration, parameters  $\hat{a}_{i,T}$  where  $i$  varies from 1-3, (table 1), in units of mass per day [mM CO<sub>2</sub> kg<sup>-1</sup> d<sup>-1</sup>],  $s_i^*$  is a Michaelis-Menton constant,  $\hat{a}_{i,T}$  is the temperature constant.

### I.4.ii. Growth

The utilization of sugar by growth is determined by the growth rates for new foliage, roots and stem:

$$(4.2) \quad \begin{aligned} GR_l &= \mathbf{a}_{gl} \cdot \mathbf{m}_l \cdot M_{lm} && \text{foliage} \\ GR_c &= \mathbf{a}_{gc} \cdot \mathbf{r}_w \cdot N \cdot w_0 \left( \sum_{n_c} V_c + 2 \cdot x_t \cdot d \right) && \text{cambium} \\ GR_e &= \mathbf{a}_{ge} \cdot \mathbf{r}_w \cdot N \cdot w_0 \sum_{n_e} V_e && \text{enlarging cells} \\ GR_m &= \mathbf{a}_{gm} \cdot \mathbf{r}_w \cdot N \sum_{n_m} V_m && \text{maturing cells} \\ GR_r &= \mathbf{a}_{gr} \cdot \mathbf{m}_r \cdot M_{rm} && \text{roots} \end{aligned}$$

where,  $\mathbf{a}_{gl}$  and  $\mathbf{a}_{gr}$  are substrate assimilation (respiration) per unit growth in the leaves and roots per day [mM CO<sub>2</sub> kg<sup>-1</sup>],  $\mathbf{a}_{gc}$ ,  $\mathbf{a}_{ge}$ ,  $\mathbf{a}_{gm}$  are substrate assimilation per unit growth in the cell wall (cambium [dividing cells], enlarging and maturing) per day [mM CO<sub>2</sub> kg<sup>-1</sup>],  $\mathbf{r}_w$  is the specific gravity of the cell wall [kg μ<sup>-3</sup>].

If 1 kg of wood tissue is equal to 0.375 kg C or 3.125·10<sup>4</sup> mM CO<sub>2</sub>, the coefficient of efficiency is:

$$(4.3) \quad \frac{3.125 \cdot 10^4}{\mathbf{a}_{gi}}$$

where,  $a_{gi}$  is the value from  $grc_i$ ,  $i$  is 1 for leaves and 5 for roots (table 1) or from  $p_{90, 91, 92}$  for cells that are dividing, enlarging or maturing (table 2).

### I.5. Water absorption by roots

The potential rate of water absorption by the roots is described as:

$$(5.1) \quad w_{max} = q \cdot f(q) \cdot m_r$$

where,  $w_{max}$  is the potential rate of water absorption by roots from a unit of soil volume [ $\text{kg m}^{-3} \text{day}^{-1}$ ],  $q$  is the “activity” of the root [ $\text{kg H}_2\text{O kg}^{-1} \text{day}^{-1}$ ],  $f(q)$  is a normalized function describing dependence of water uptake on soil water content  $q$  [v/v]. This function takes a trapezoidal form (figure 5.1) (similar to the temperature dependence curve, equation 2.4) with parameters  $q$  for field capacity,  $q_{min}$  for wilting point,  $q_1$ - $q_2$  for the range of optimal soil moisture,  $q_{max}$  for saturation when soil oxygen is absent and water uptake cannot take place.

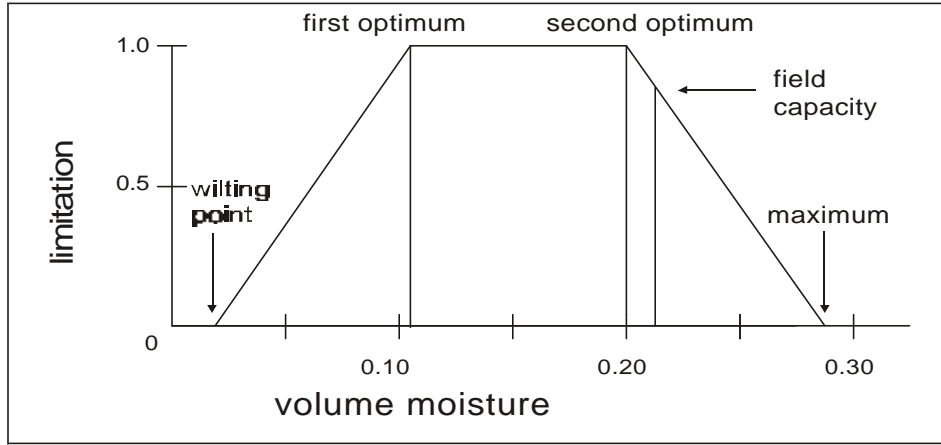


**Figure 5.1.** Five parameters are used to define the moisture available to the roots: 1) wilting point, 2) the first optimum (lowest soil moisture when rate reaches optimum), 3) second optimum (highest soil moisture when rate is optimum), 4) field capacity and 5) maximum when low soil oxygen prohibits uptake. Similar parameters are used to express the limiting effects of temperature on different processes or features of the ring.

Parameters describing the soil volume vary as a function of the annual leaf mass estimated from sapwood volume (Monserud and Marshall, 1999) and tree age. If the root system has mass  $M_r$ , the tree occupies a soil volume with a surface area,  $A$  ( $p_{15}$ ) and a depth,  $h$  ( $p_{14}$ ), ( $v_s = A \cdot h$ ) the potential water absorption by root of the tree will be:

$$(5.2) \quad W_{max} = q \cdot f(q) \cdot m_r \cdot v_s = q \cdot f(q) \cdot M_r$$

The tree water balance is calculated depending upon the potential rates of absorption,  $W$ , loss of water due to transpiration,  $Tr$ , and resistance of the leaves  $R^c = I R^w$  (where  $I$  is the transformation coefficient from water resistance into  $\text{CO}_2$  diffusion resistance). If  $Tr^p \ll W_{max}$  then  $W = Tr = Tr^p$ ,  $R^w = R_{min}$ . If  $Tr^p \approx W_{max}$  then  $Tr = W_{max}$ ,  $R^w = R_{min} \cdot Tr^p / W_{max}$  ( $R^w \ll R_{max}$ ). The value  $R^c = I \cdot R^w$  is used to calculate the photosynthetic rate (see equation 2.1).

If photosynthesis is not limited by CO<sub>2</sub>, resistance is controlled by the rate of photosynthesis (equation 2.4) and:

$$(5.3) \quad W = Tr = Tr^p \cdot \frac{I \cdot R^w}{R_p^c}$$

## I.6. Growth

### I.6.i. Leaves

The foliage of the tree is described as leaves of different age. The foliage produced during the current year has mass  $M_{l0}(t)$ , the one year-old leaves have mass  $M_{l1}(t)$  etc.

The mass of meristematic cells ( $M_{lm}$ ) is proportional to the potential mass of new foliage  $M_{l0}^*$ ,  $M_{lm} = h_l M_{l0}^*$ . The dynamic of foliage growth is:

$$(6.1) \quad \begin{aligned} \frac{dM_{l0}}{dt} &= m_l \cdot M_{lm} - I_{l0} \cdot M_{l0} \\ \frac{dM_{li}}{dt} &= -I_{li} \cdot M_{li} \end{aligned}$$

where,  $I_{li}$  is the rate of leaves lost at age  $i$ ,  $m_l$  is the rate of new foliage growth by foliage meristem. As mentioned earlier  $M_l$  is constant, at this stage of the model development, which means that  $m_l M_{lm} = \sum I_{li} M_{li}$ . The photosynthetic active foliage is  $M_l = \sum M_{li}$ . The rate of leaf growth is:

$$(6.2) \quad m_l = m_0 (1 - M_{l0}/M_{l0}^*) F_l(s, T, W)$$

where,  $M_{l0}^*$  is the potential mass of new foliage,  $F_l$  is a normalized function relating the growth rate to limiting conditions of substrate concentration, temperature and water balance.

### I.6.ii. Stem

The term stem includes all parts of the tree in which the growth is based on secondary growth in the cambium. This includes branches, the main stem and coarse roots. The living cells in the stem include various cellular types such as ray cells, parenchyma, living phloem cells and the population of the cambial initials. As mentioned above, it is assumed that the ratio of meristem cells (cambial initials) to all other living cells is constant (the number or mass of cambial initials is constant and proportional to the mass of all living cells in the stem,  $M_s$ ).

The differentiation of mature tracheids elements is modeled for one radial file that is assumed to be characteristic for all radial files in the tree. Growth in the radial file involves division of the cambial initials and xylem mother cells in the cambial zone, followed by enlargement and wall thickening in zones of enlargement and maturation. As a cell grows, sugar is converted to cell wall material. This consumption of sugar is included as one of the carbon sinks along with the growth and maintenance respiration of all other living cells of the tree (see section 4).

The production of new xylem cells is a complex process related in part to the mass of cambial initial cells. The number of cells in the radial file includes:

one initial cell	- $n_i$
xylem mother cells	- $n_c$
elongating cells	- $n_e$
maturing cells	- $n_m$

Each cell in the radial file is characterized by values of several parameters. The controls to these are input parameters  $b_i$  in file CAMBINI (table 2).

$j$  - is the position of each cell in the radial file. The initial cell is position 1 and those derived from it are numbered by their actual position in the file at the current time.

$x_j$  - is the cell size in the radial direction. The tangential cell size is assumed constant and is entered as a parameter of the model.

$w_j$  - is the cell wall area in cross section.

Cell size is the most important characteristic in determining the behavior of each cell. While in the cambium zone, each cell increases in size until it reaches a maximum size and divides (moves through the cell cycle). The resulting daughter cells are one half the maximum cell size after each cell division. The innermost cells in the cambial zone lose their ability to divide and enter the enlargement phase, where the cell size continues to increase but at a diminishing rate. When the rate of size increase reaches a critical value, the cell loses its ability to enlarge and enters the zone of maturation, but where the cell wall is thickening wall synthesis continues until the cell dies.

#### I.6.ii.a. Division of cambium cells

Unless the cambium is dormant, all initial and mother cells pass through the phases of the cell cycle: G1, S, G2 and M at a constant growth rate,  $V_o$ , ( $b_{23}$ ). The size of each cell when it enters a particular phase is  $D_{G1}$ ,  $D_s$ ,  $D_{G2}$  and  $D_m$  ( $b_{10}$  -  $b_{13}$ ). When the cell is in phase G1, the rate of division,  $V_c$ , varies as a function of distance from the initial cell and limiting conditions. The duration of the full cell cycle with a constant  $V_c$  will be:

$$(6.3) \quad \frac{D_{G1} - D_m / 2}{V_c} + \frac{D_m - D_{G1}}{V_o}$$

However,  $V_c$  is not constant but changes with position in the cellular file (figure 6.2), varying limiting conditions and controlling factors that change through time. As a result, duration of the cell cycle cannot be expressed as a simple equation.

The rate of cell growth in position  $j$  is a function of the distance,  $y$ , from initial cell, and is related to limiting conditions and numbers of other growing and maturing cells as follows:

(6.4)

$$V_c = b_{22} \cdot (b_{25} - (60 - y)) \cdot b_{24} \cdot \left( \frac{x}{x + b_{28}} \right) \cdot F_c(s_s, T)$$

where,  $V_c$  is the growth rate of cell in position  $j$  (figure 6.2),  $b_{24}$  is the slope regulating the increasing growth rate of cambial cells across the cambial zone,  $x$  is the sum of the cell sizes in the division, enlargement and maturation zone,  $b_{28}$  is the ring width of growing cells (microns) when the slope of the division rate is  $\frac{1}{2}$  the maximum value,  $b_{22}$  is a scalar of growth rate, and  $b_{31}$  is the sensitivity of growth to  $C_t$  ( $b_{31} > 1$ ).

The relationship between the rate of growth  $V_c$  and  $x$  of the differentiating cells is used to control the rate of division of the cambial

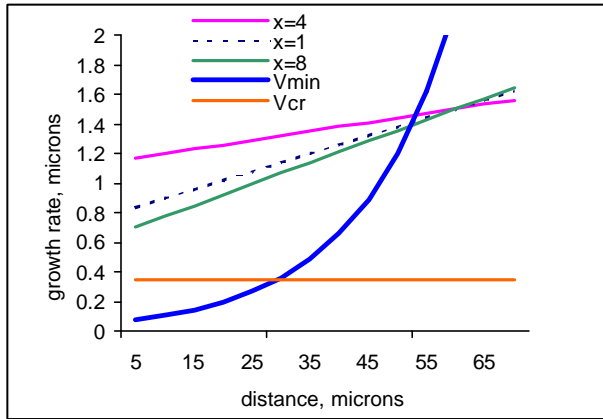


**Figure 6.3.** At the beginning of the season when there is only one cambial cell in position 1 ( $x=1$ ), the growth rate is high. As cell division produces more cambial cells ( $x=4$  and  $x=8$ ) the growth rates decline. In this example no external factors are limiting ( $b_{28}=2$ ), the growth rates,  $V_{min}$  and  $V_{cr}$  are the same as in figure 7.2.

other phase, the cell continues to divide until it completes the division process. The function  $V_{min}$  is determined as:

$$(6.5) \quad V_{min} = b_{22} \cdot \text{EXP}[b_{26}(y - b_{27})(1 + (b_{32} - 1)C_t) / b_{32}]$$

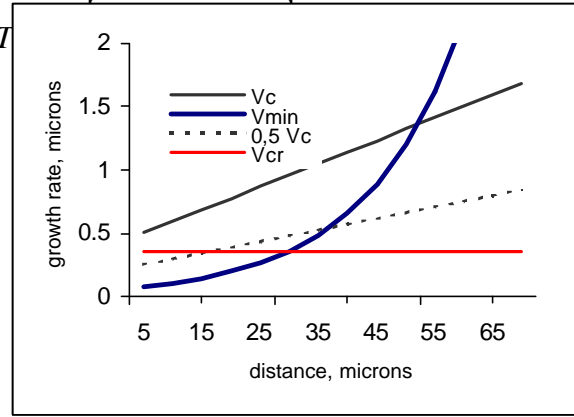


**Figure 6.2.** The growth rate,  $V_c$  increases with increasing  $j$ , the cell number sequence starting with the cambial initial. The growth rates of cells not limited by environmental and growth-regulating factors ( $V_c$ ) grow most rapidly. Cells that are limited, such as  $0.5 V_c$  grow more slowly. When rates decline below  $V_{min}$  the cells lose their ability to divide. When the rate reaches  $V_{cr}$  the cambium becomes dormant. ( $b_{22}=0.5187$ ,  $b_{24}=0.035$ ,  $b_{25}=2.9$ ,  $b_{28}=0$ ,  $b_{26}=0.0$ ,  $b_{27}=36$ ,  $V_{cr}=0.35$ ).

initial and mother cells at the beginning of the growing season when few cambial cells are present (figure 6.3) through a feed back loop,  $F_c$  is a normalized function ranging from 0 to 1, and  $C_t$  (0 to 1) is the control from the rate of growth in the crown.

We changed the relationship involving position of the cell to distance from initial cell. In the previous version the number of cells in the cambium sometimes fluctuated so widely from day to day as to make the model unstable. This change from position to distance increased the stability of the model.

The cell leaves the zone of cell division and enters into the enlargement stage if its  $V_c < V_{min}$  (figure 6.2 and 6.3) and the cell is in the  $G_1$  phase of the division cycle. If the cell is in any

where,  $b_{22}$  is a scalar of growth rate,  $b_{26}$  is a coefficient of the equation,  $b_{32}$  is the sensitivity of growth to  $C_t$  (when  $b_{32} > 1$ ). The relationship of  $V_{min}$  by  $C_t$  was added because it was thought that growth regulators produced in the crown as a function of the rate of crown growth may also influence  $V_{min}$ , which determines when the dividing cells begin to enlarge. If  $C_t$  has no effect  $b_{32} = 1$ .

Cell division will stop reversibly (the cambium becomes dormant) for all cells in phase G1 if  $V_c < V_{cr}$  ( $V_{cr} = b_{22} b_{21}$ ) or day length less than  $b_{29}$ .

### I.6.ii.b. Cell enlargement

The dynamics for enlargement of cells is described as:

$$(6.6) \quad d_j(t + \mathbf{D}) = d_j(t) + V_e \mathbf{D}$$

where,  $d_j(t)$  is the radial size of cell in position  $j$  at time  $t$  [microns];  $t_0$  is time step of calculation [day];  $V_e$  is the growth rate [microns/day].

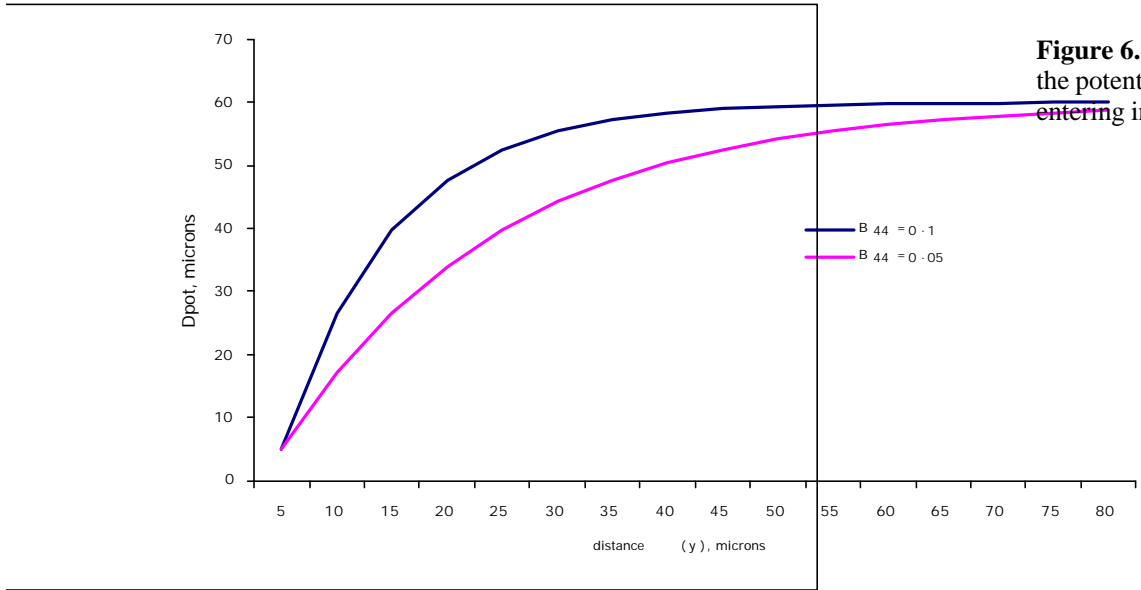
The growth rate of cells in the enlargement stage is calculated as:

$$(6.7) \quad V_e = b_{46} (dpot_j - d_j(0)) \text{EXP}(-b_{46} \tau) F_e(s_s, T, W) (1 + (b_{51} - 1)C_t) / b_{51}$$

where,  $b_{46}$  is the parameter that scales the decline in rate as a function of time,  $dpot_j$  is the potential cell size,  $d_j(0)$  is the initial cell size at the time when the cell enters the enlargement stage,  $\tau$  is the time that cell  $j$  spends in the enlargement stage. The remaining terms on the right represent the controls of environment and crown growth. The potential cell size is a function of the distance ( $y$ ) from the initial cell (equation 6.4) when cell  $j$  started enlarging:

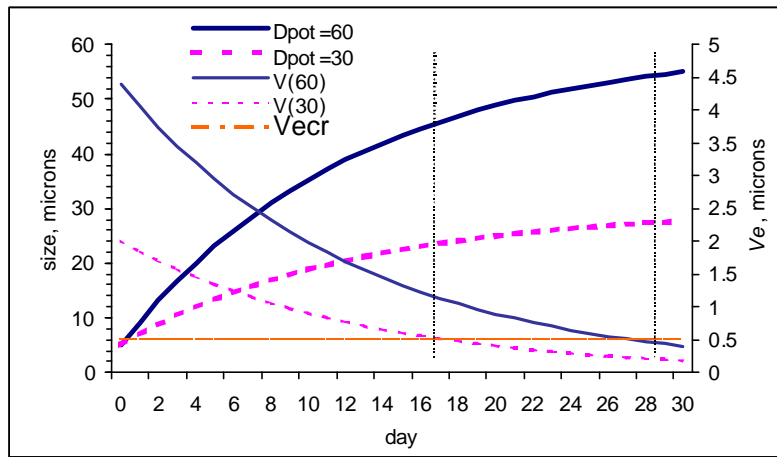
$$(6.8) \quad dpot_j = d_{max} - (d_{max} - d_{min}) \text{EXP}(-b_{44}(y - b_{45}))$$

where,  $b_{44}$  and  $b_{45}$  are parameters,  $d_{max}$ ,  $d_{min}$ , are the maximum and minimum cell size ( $b_2$ ,  $b_1$ ).



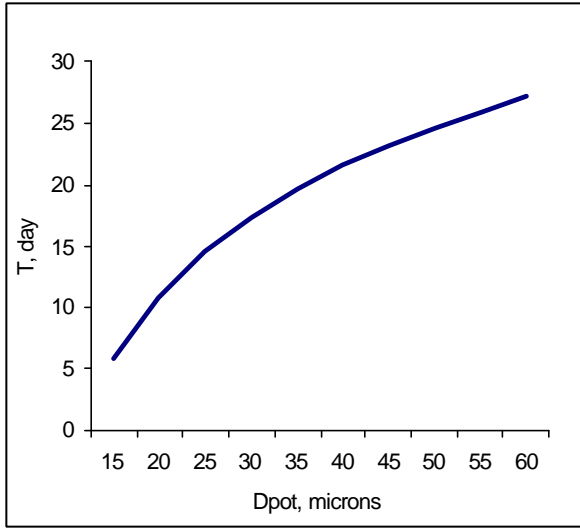
**Figure 6.4.** The relationship of the potential cell size on position entering in the enlargement stage.

Figure 6.4 shows the control of  $b_{44}$  on the potential cell size. The smaller the value of  $b_{44}$  the greater the effect of distance ( $y$ ) across the cambial zone on maximum cell size. If  $b_{44}$  is 0.1 or smaller and cambial growth is slow with few dividing cells present ( $y$  is small), the potential enlargement will be reduced. This would occur in the case of a mid-summer drought. As the number of cells in the dividing zone declines, the ability for cells to enlarge is correspondingly reduced. Parameter  $b_{45}$  is the critical width of the cambial zone at which  $y$  begins to influence the potential cell size. Below that width the size of the dividing layer has no effect on potential cell size.



**Figure 6.5.** The dynamics of cell growth (potential cell size 60 and 30 microns) and the growth rate  $V_e$  ( $b_{46}=0.08$ ;  $dj(0)=5.0$ ).

Parameter  $b_{46}$  is critical for the dynamics of the enlargement as it scales the rate of declining growth as a function of time ( $t$ ). At optimal conditions cell size increases as  $D=Dpot-(Dpot-Do)EXP(-b_{46} t)$  at a decreasing rate through time (figure 7.5). However the effect of parameter  $b_{46}$  is limited by  $Vcr$  ( $b_{42}$ ), which is the threshold rate when enlargement stops and the cell wall thickening begins. Thus the duration of enlargement is  $T=1/b_{46} * \ln(b_{46}/Vcr*(Dpot-Do))$  (see figure 6.6). If one wishes to restrict the number of days in enlargement to a maximum of 30 to 40 days, it is necessary to change  $b_{46}$  and  $b_{42}$  ( $Vcr$ ) together.



**Figure 6.6.** The dependence duration of enlargement ( $T$ ) on potential cell size ( $D_{pot}$ ).

### I.6.ii.c. Cell maturation

The dynamics of cell wall synthesis and wall thickening are similar to those of cell enlargement. The rate of cell wall synthesis is:

$$(6.9) \quad w_j(t + \mathbf{D}) = w_j(t) + V_m \mathbf{D}, \quad w_j(0) = w_{min}$$

where,  $w_j$  is the cell wall thickness of the  $j^{\text{th}}$  cell [mkm],  $V_m$  is the rate of cell wall synthesis [mkm day<sup>-1</sup>]. The rate of cell wall synthesis is calculated as:

$$(6.10) \quad V_m = b_{64} (wpot_j - w_{min}) \text{EXP}(-b_{64} \mathbf{t}) F_m(ss, T, W) (1 + (b_{67} - 1)C_i) / b_{67}$$

where,  $b_{64}$  is a parameter that scales the decline in rate as a function of time,  $wpot_j$  is the potential cell wall thickness,  $w_{min}$  is the minimum cell-wall thickness ( $b_4$ ),  $\mathbf{t}$  is the time that cell  $j$  spends in the maturation stage. The remaining terms on the right represent the controls of environment and crown growth. The potential cell wall thickness is a function of size of the  $j^{\text{th}}$  cell.

$$(6.11) \quad wpot_j = \text{MIN}[w_{min} - (w_{min} - w_{max}) \text{EXP}(-b_{63}(d_j - d_{min})), d_j (1 - l_{min}) / 2]$$

where,  $w_{max}$ ,  $w_{min}$ ,  $d_{min}$  are the parameters ( $b_4$ ,  $b_5$ ,  $b_1$ ) that define the potential cell size. The potential cell wall ( $wpot_j$ ) can not be bigger then  $d_j (1 - l_{min}) / 2$  ( $l_{min}$  is minimum of lumen size

expressed as a percentage). In fact this function describes the boundary of late and early wood cells shown in figure 6.7.

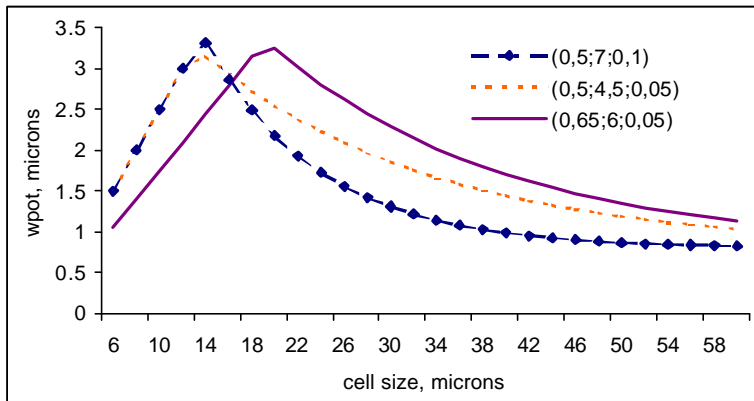


**Figure 6.7.** The relationship of the potential cell wall thickness ( $w_{pot}$ ) on the cell size at different parameters. (in brackets:  $l_{min}$ ,  $w_{max}$ ,  $b_{63}$ ).

Wall synthesis irreversibly stops when  $V_m$  less than  $V_{mcr}$  ( $b_{62}$ ). Note that the equations for wall thickening are the same as those for enlargement. At optimal conditions wall synthesis is  $w = w_{pot} - (w_{pot} - w_{min}) \text{EXP}(-b_{64} t)$  (figure 6.8). The duration in the wall thickening stage,  $T$ , is  $T = 1/b_{64} \ln(b_{64}(w_{pot} - w_{min})/V_{mcr})$ . As you can see on figure 6.8 the parameter  $b_{64} = 0.1$ , which was used in one version tuning, causes fast rates of wall thickening and the duration is only 30 and 22 days for cells with potential wall thickness 4 and 2 microns. With increasing value of  $b_{64}$  the rate of thickening is faster and duration during which cells remain in the thickening zone reduced. As in enlargement it is best to change  $V_{mcr}$  and  $b_{64}$  together to arrive at a reasonable time, for maximum  $w_{pot}$  (figure 6.8).

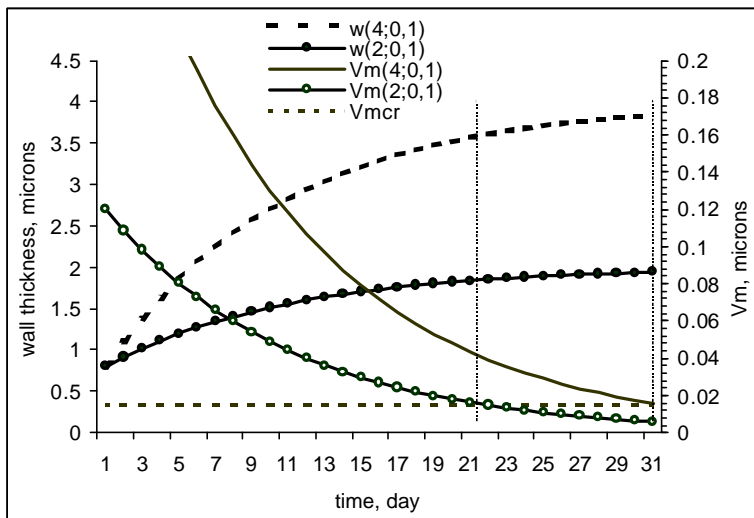


**Figure 6.8.** The rate ( $V_m$ ) and dynamics of cell wall thickness ( $w$ ). In brackets:  $w_{pot}$ ,  $b_{64}$ .

### 1.6.iii. Roots

The root system is treated as a carbon sink using substrate during the growing process as it produces new mass (surface area) enabling water uptake from the soil. Water uptake is a function

of the mass of living cells in the fine roots while growth of these roots is a function of the root meristematic tissue. The growth of roots is simulated in the model as:

$$(6.11) \quad \frac{dM_r}{dt} = \mathbf{m}M_{rm} - \mathbf{I}_r M_r$$

where,  $\mathbf{m}$  is the rate of fine root production by the root meristem, which varies as a function of limiting factors,  $M_{rm} = \mathbf{h}_r M_r$  is the mass of root meristem. There is no dynamic of root growth in the current version of the model, which implies that  $\mathbf{m}M_{rm} = \mathbf{I}_r M_r$ .  $\mathbf{m} = \mathbf{m}_0 F_r(s_r, T, W)$  and  $\mathbf{I}_r$  is the rate of mortality of roots.

## I.7. Allocation, Redistribution and Storage of substrate

The dynamics of substrate content, in the leaves is:

$$(7.1) \quad \frac{dS_l}{dt} = P - Rm_l - GR_l - \mathbf{x}_{ls}(s_l - s_s)$$

in the stem is:

$$(7.2) \quad \frac{dS_s}{dt} = \mathbf{x}_{ls}(s_l - s_s) - Rm_s - GR_c - GR_e - GR_m - \mathbf{x}_{sr}(s_s - s_r)$$

and in roots is:

$$(7.3) \quad \frac{dS_r}{dt} = \mathbf{x}_{sr}(s_s - s_r) - Rm_r - GR_r$$

where,  $S_l$ ,  $S_s$  and  $S_r$  are the substrate content [mM CO<sub>2</sub>] in the leaves, stem and roots respectively, likewise  $s_l$ ,  $s_s$  and  $s_r$  are substrate concentrations [mM CO<sub>2</sub> kg<sup>-1</sup>] in the leaves, stem and roots, and  $\mathbf{x}_{ls}$  and  $\mathbf{x}_{sr}$  are coefficients of diffusion for the substrate from leaves to the stem and from the stem to the roots [kg t<sup>-1</sup>].

Daily allocation and redistribution subroutines control the relative distribution of sucrose among growth and storage at the leaves, stem and roots and usage by the three main sinks: respiration, growth and storage. Sucrose is assumed to be completely mobile throughout the tree each day, in accordance with studies that have shown that the distance of assimilate transfer is not a major factor limiting growth (Wardlaw, 1990), whereas stored starch is assumed to mobilize only when sucrose is fully depleted. Preferential use of sucrose is supported by studies with barley and sugar beet (Fondy and Geiger, 1982) that indicate starch mobilization in leaves at the beginning of the night was restricted until after sucrose in the leaves was reduced.

At the beginning of each day the cumulative amount of newly produced sucrose and any sucrose left from the previous day represents the new sucrose volume. Each sink and location is prioritized such that new photosynthate formed in the leaves is utilized in the following order:

- 1) Respiration in the a) leaves, 

- |                   |            |                                    |
|-------------------|------------|------------------------------------|
|                   | b) stem,   |                                    |
|                   | c) roots.  |                                    |
| 2) Growth in the  | d) leaves, | <i>Carbon allocation 'cascade'</i> |
|                   | e) stem,   |                                    |
|                   | f) roots.  |                                    |
| 3) Storage in the | g) leaves, |                                    |
|                   | h) stem,   |                                    |
|                   | i) roots.  |                                    |

Each day instantly available photosynthate 'trickles down' the *carbon allocation cascade* being depleted at each level by the amount of the specific sink, where Sink Strength = Sink Size × Sink Activity (Taiz & Zeiger, 1991, p.171). The process continues until the sucrose is either completely utilized or the final sink (storage in the roots - i) is realized.

A percentage of the sucrose remaining at the end of the day will be allocated to starch. As a first approximation we assume a set daily rate of conversion from total sucrose to starch that is determined by the user (between 0 and 100%); for the data shown here this is 80%. It is realized that this rate will vary over time and among trees, and this may prove a key area of improvement in future model revisions. The relative proportions of sucrose that are converted to starch at each location within the tree (leaves, stem and roots) are determined by the relative volume of active cells in each location. This provides a link between reserve dynamics and growth activity, which is supported by observations on other tree species (Hansen 1967; Lacoite *et al.* 1993).

### I.8. Soil water

The content of water in soil of volume  $v_s = A_s h$  is calculated each day as:

$$(8.1) \quad \frac{d\Theta}{dt} = A_s \min(Pr(t)a_1, Pr^*) - W - a_2\Theta$$

when  $q_v \ll q \ll q$

$$q = \frac{\Theta}{v_s}$$

where,  $\Theta$  is the water content in soil volume  $v_s$  [kg],  $q$  is soil moisture [kg/ m<sup>3</sup>],  $Pr(t)$  is the precipitation [mm day<sup>-1</sup>],  $Pr(t)(1-a_1)$  is the interception of precipitation by the crown ( $a_1$ ),  $Pr(t)a_1$  is the precipitation that goes into the soil. If  $Pr(t)a_1$  is greater than the value  $Pr^*$ , there will be surface runoff equal to  $Pr(t)a_1 - Pr^*$ . Additional loss of water occurs when the soil water content exceeds field capacity, and  $q$ .  $a_2\Theta$  is the rate of infiltration of water from the soil.

## I.9. Isotope calculations

### I.9.i. Carbon

#### I.9.i.a. Photosynthate

Utilizing the model estimates for average daily concentration of CO<sub>2</sub> inside the leaves ( $C_i$ ), the basic equation of carbon isotope fractionation ( $\delta^{13}\text{C}$ ) in C<sub>3</sub> plants (Farquhar *et al.*, 1982) has been used to model the  $\delta^{13}\text{C}$  composition of photosynthate:

$$(9.1) \quad \mathbf{d}^{13}C_p = \mathbf{d}^{13}C_a + \mathbf{a} \left( 1 - \frac{C_i}{C_a} \right) + \mathbf{b} \left( \frac{C_i}{C_a} \right) + r$$

where,  $\mathbf{d}^{13}C_p$  is the  $\delta^{13}\text{C}$  of photosynthate,  $\mathbf{d}^{13}C_a$  is the  $\delta^{13}\text{C}$  of ambient atmospheric CO<sub>2</sub>,  $\mathbf{a}$  ( $\approx -4.4\%$ ) is the maximum fractionation of  $\delta^{13}\text{C}$  resulting from the diffusion of CO<sub>2</sub> through leaf boundary air layers,  $\mathbf{b}$  ( $\approx -29\%$ ) is the maximum fractionation of  $\delta^{13}\text{C}$  resulting from the biochemical reactions of carboxylation and PEP carboxylase (O'Leary, 1981),  $C_i$  is the leaf internal CO<sub>2</sub> concentration,  $C_a$  is the ambient atmospheric CO<sub>2</sub> concentration, and  $r$  is fractionation resulting from respiration (equations 9.2 and 9.3). Values of atmospheric CO<sub>2</sub> concentration and  $\delta^{13}\text{C}$  composition are estimated as annual values from ice core and flask measurements, where flask measurements are averaged for the summer months between May and October (Hemming *et al.*, 1998). No account is presently taken of intra-annual variations in atmospheric CO<sub>2</sub> concentration and  $\delta^{13}\text{C}$  composition.

The diurnal respiration fluxes estimated for each site within the tree (leaves, stem and roots) (see section I.4), are used to estimate  $\delta^{13}\text{C}$  fractionation from respiration at each site ( $r$  in equation 9.1). For the stem and roots it is assumed that the only form of respiration is dark respiration, which is modeled as follows:

$$(9.2) \quad \mathbf{d}^{13}C_{dr} = \frac{(\mathbf{e} \cdot R_d)}{\mathbf{k}} \Big/ C_a$$

where,  $\mathbf{d}^{13}C_{dr}$  is the  $\delta^{13}\text{C}$  fractionation during dark respiration,  $\mathbf{a}$  is the maximum fractionation from dark respiration,  $R_d$  is the rate of dark respiration,  $\mathbf{e}$  is a complex parameter (refer to Farquhar *et al.*, 1982) and  $C_a$  is ambient CO<sub>2</sub> concentration.

For the leaves only, the  $\delta^{13}\text{C}$  fractionations resulting from both dark and photo respiration are modeled using:

$$(9.3) \quad \mathbf{d}^{13}C_r = \frac{(\mathbf{r} \cdot \mathbf{g} + \mathbf{e} \cdot R_d)}{\mathbf{k}} \Big/ C_a$$

where,  $\mathbf{d}^{13}C_r$  is the  $\delta^{13}\text{C}$  fractionation during dark and photo respiration,  $\tilde{n}$  is the maximum photo respiration fractionation and  $\tilde{a}$  is the CO<sub>2</sub> compensation point.

To translate the modeled photosynthate  $\delta^{13}\text{C}$  compositions to  $\delta^{13}\text{C}$  compositions for the whole leaf, stem and root daily estimates of carbon sink strength at each site and the source strength of presently formed photosynthate are used to determine the relative proportions of  $\delta^{13}\text{C}$  contributed from presently formed photosynthate and remobilized starch. The  $\delta^{13}\text{C}$  compositions of present photosynthate and stored starch in each location are estimated (see section I.7), and therefore an isotopic mass balance of present and stored photosynthate and starch can be used to estimate whole leaf, stem and root  $\delta^{13}\text{C}$  composition:

$$(9.4) \quad \mathbf{d}^{13}\text{C}_w \cdot Si_w = \mathbf{d}^{13}\text{C}_p \cdot So_p + \mathbf{d}^{13}\text{C}_s \cdot So_s$$

where,  $Si$  and  $So$  are the carbon sink and source and the subscripts  $w$ ,  $p$  and  $s$  indicate the whole sink area, photosynthate and starch respectively.

Daily estimates of sink strength and  $\delta^{13}\text{C}$  composition for the stem are partitioned to specific cells within an annual ring using the model of cambial development (see section I.6), such that as each cell grows its  $\delta^{13}\text{C}$  composition is modified by the  $\delta^{13}\text{C}$  composition of the additional stem  $\delta^{13}\text{C}$ . The final cell whole wood  $\delta^{13}\text{C}$  composition therefore reflects the  $\delta^{13}\text{C}$  compositions and proportions of the sources (photosynthate and starch) and the timing during which these sources are utilized in the formation of cell walls.

### *I.9.ii Oxygen and Hydrogen*

The oxygen and hydrogen isotopic compositions ( $\delta^{18}\text{O}$  and  $\delta\text{D}$ ) of tree ring cellulose are modeled using the additional inputs of the  $\delta^{18}\text{O}$  and  $\delta\text{D}$  of precipitation and atmospheric water vapor. Three main steps are taken to translate these inputs to cellulose isotopic composition:

- a. a basic soil water mixing model is used to mix the isotopic compositions of precipitation with existing soil water,
- b. an established model is utilized to estimate evaporative enrichment in the leaf, and
- c. mixing factors are used to estimate the degree of mixing between waters in the leaf and stem.

These steps are outlined below.

#### I.9.ii.a. Soil Water / Xylem Water

A basic soil-water mixing model is constructed to calculate daily values of  $\delta^{18}\text{O}$  and  $\delta\text{D}$  of soil water. With a precipitation event the  $\delta^{18}\text{O}$  and  $\delta\text{D}$  of the precipitation is combined with the isotopic compositions of the existing soil water in proportions comparable with the amounts of existing soil water (calculated per  $\text{m}^2$ ) and additional precipitation (figure 9.5), as follows:

$$(9.5) \quad \mathbf{d}_{\text{SW}} = \mathbf{d}_{\text{SW-1}} \cdot \left( \frac{V_{\text{SW}}}{V_{\text{SW}} + V_{\text{PREC}}} \right) + \mathbf{d}_{\text{PREC}} \cdot \left( 1 - \frac{V_{\text{SW}}}{V_{\text{SW}} + V_{\text{PREC}}} \right)$$

$V_{\text{PREC}}$

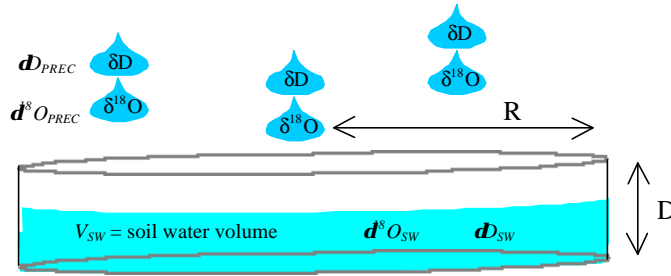


**Figure 9.5.** Schematic of mixing model for soil water isotope composition.

where,  $V_{PREC}$  and  $V_{SW}$  are the volumes of precipitation falling on the soil area and of existing soil water,  $R$  is the radius of the horizontal extension of roots (of a circular “footprint” of roots centered on the tree bole),  $D$  is root depth,  $d_{SW}$  and  $d_{SW-I}$  are the new isotopic composition ( $\delta^{18}O$  or  $\delta D$ ) of soil water and the estimation of soil water from the previous calculation step, and  $d_{PREC}$  is the isotopic composition of additional precipitation. The isotopic composition of soil water changes when soil water increases but does not change when it decreases. The existing parameter of maximum precipitation rate is utilized such that above the specified maximum precipitation rate water is lost to runoff and isotopic mixing in the soil does not occur.

At present, the soil water-mixing model contains no fractionation by evaporation in the surface soil layers and it is assumed that the water taken up by the roots is a representative sample of the whole soil water pool.

### I.9.ii.b. Leaf Water Model

During uptake of soil water by roots and its translocation in the xylem to the leaves it is assumed that isotopic fractionations are insignificant. It is also assumed that, above the critical soil moisture threshold, the soil water of each day is available to the leaves the following day. Therefore, the xylem water entering the leaves on a specific day has  $\delta^{18}O$  or  $\delta D$  compositions equal to that of bulk soil water of the previous day.

The isotopic composition of leaf water at the sites of maximum evaporation (sub-stomatal cavities) is estimated using a basic model of water surface fractionation during evaporation (Craig and Gordon, 1965) adapted to include leaf boundary layers (Flanagan and Ehleringer, 1991):

$$(9.6) \quad d_{LW} = \mathbf{a}' \left[ \mathbf{a}_k \cdot d_{XW} \cdot \left( \frac{e_i - e_b}{e_i} \right) + \mathbf{a}_{kb} \cdot d_{XW} \cdot \left( \frac{e_b - e_a}{e_i} \right) + d_{RH} \cdot \left( \frac{e_a}{e_i} \right) \right]$$

where,  $d_{LW}$  is the  $\delta^{18}O$  or  $\delta D$  of leaf water,  $\mathbf{a}'$  is the liquid-vapor isotopic fractionation factor ( $\delta^{18}O=1.0088$ ,  $\delta D=1.079$ ),  $\mathbf{a}_k$  is fractionation due to diffusion of  $H_2O$  in air ( $\delta^{18}O = 1.0285$ ,  $\delta D=1.025$ ),  $d_{XW}$  is the  $\delta^{18}O$  or  $\delta D$  of xylem water,  $e_i$ ,  $e_b$ ,  $e_a$  are vapor pressures of air at the leaf intercellular cavity, leaf boundary and ambient atmosphere,  $\mathbf{a}_{kb}$  is fractionation due to diffusion of  $H_2O$  through the leaf boundary layer ( $\delta^{18}O = 1.0189$ ,  $\delta D=1.017$ ), and  $d_{RH}$  is the  $\delta^{18}O$  or  $\delta D$  of atmospheric water vapor.

Equation 9.7 provides an option to mix the incoming xylem water with the isotopically enriched leaf water estimated in equation 9.2.

$$(9.7) \quad \mathbf{d}_{LW_{bulk}} = (\mathbf{d}_{LW} \cdot f) + (\mathbf{d}_{XW} \cdot (1 - f))$$

where,  $\delta_{LW_{bulk}}$  is the  $\delta^{18}\text{O}$  or  $\delta\text{D}$  of bulk leaf water,  $\delta_{LW}$  is the  $\delta^{18}\text{O}$  or  $\delta\text{D}$  of leaf water calculated in equation 9.6,  $f$  is the fraction of bulk leaf water subjected to evaporative enrichment, and  $\delta_{XW}$  is the  $\delta^{18}\text{O}$  or  $\delta\text{D}$  of xylem water.

### I.9.ii.c. Photosynthate and cellulose

Photosynthates that are formed in the chloroplast and cytosol of the leaves retain a component of the  $\delta^{18}\text{O}$  and  $\delta\text{D}$  compositions of the leaf water medium in which they were formed. However, autotrophic (dark) and heterotrophic (light) reactions may change these compositions significantly.

Assuming that the  $\delta^{18}\text{O}$  and  $\delta\text{D}$  compositions of bulk leaf water (estimated in equation 9.7) are representative of the leaf water medium in which photosynthates are formed, and that these compositions are subsequently modified by known autotrophic and heterotrophic fractionations, equations 9.8 and 9.9 are used to estimate photosynthate and cellulose  $\delta^{18}\text{O}$  and  $\delta\text{D}$  (non-exchangeable, carbon bound  $\delta\text{D}$  only):

$$(9.8) \quad \mathbf{d}_{PS} = \mathbf{d}_{LW_{bulk}} + E_{auto} + E_{het}$$

where,  $\mathbf{d}_{PS}$  is the  $\delta^{18}\text{O}$  or  $\delta\text{D}$  of photosynthate exported from the leaves,  $\mathbf{d}_{LW_{bulk}}$   $\delta^{18}\text{O}$  or  $\delta\text{D}$  of bulk leaf water and  $E_{auto}$  is autotrophic fractionation (27‰ for  $\delta^{18}\text{O}$  (Sternberg & DeNiro, 1983), -171‰ for  $\delta\text{D}$  (Yakir & DeNiro, 1990)) and  $E_{het}$  is heterotrophic fractionation (0‰ for  $\delta^{18}\text{O}$ , 158‰ for  $\delta\text{D}$  (Yakir & DeNiro, 1990)).

$$(9.9) \quad \mathbf{d}_C = (\mathbf{d}_{XW} \cdot f) + (\mathbf{d}_{PS} \cdot (1 - f))$$

where,  $\mathbf{d}_C$  is the  $\delta^{18}\text{O}$  or  $\delta\text{D}$  (non-exchangeable) of cellulose,  $f$  is the fraction of H and O exchanged with xylem water (parameters isoH(3) and isoO(3)) and  $\mathbf{d}_{PS}$  is the  $\delta^{18}\text{O}$  or  $\delta\text{D}$  of photosynthate (from equation 9.8).

## EXTERNAL INPUTS

### II.1. Daily Meteorological Data

Daily meteorological data from Palisades Ranger Station meteorological station in the Santa Catalina Mountains near Tucson, Arizona (~4km from the study site - see section C.3.) were

used as the fundamental inputs for the theoretical equations described above. The records of temperature (max and min) and precipitation from this station are available for the period 1965 to 1981. Linear regression relationships between these records and those from various meteorological stations within ~20km of this location were used to fill gaps and extend the records to cover ~100 years (1893/5 - 1999). The decision to use particular records or averages of various records for this reconstruction was made by correlating the various records available (and their averages) with the Palisades record, for the period 1965 to 1981. Those records with the highest correlations that cover the time period required for reconstruction were chosen. Gaps in each of the individual records were filled using regression relationships with the most highly correlated nearby record covering the required period.

The following sections detail the meteorological records and regression relationships used to construct the Palisades Ranger Station record for each parameter and without gaps.

### *II.1.i. Maximum Temperature*

(in °F , model converts to °C)

Actual data from Palisades: 1965-1981, includes gaps

Reconstructed data for Palisades: 1893-1964, 1982-1999, plus gaps in original record

Records and regression relationships used for various time periods:

Using Oracle record:

$$\mathbf{1893 - 1948:} \quad \mathbf{y = 0.9302x - 9.9979} \quad \mathbf{R^2 = 0.8975}$$

*where x = Oracle max temperature.*

Using Tucson Farm record (starts at 1949):

**1949-1964 and 1982-2000 plus gaps in Palisades record between 1965-1981:**

$$\mathbf{y = 0.9458x - 15.236} \quad \mathbf{R^2 = 0.9231}$$

*where x = average of Oracle and Tucson Farm max temperature.*

Gaps in the Oracle record:

For the periods 1894-1964 and 1982-1999 gaps in the Oracle record were filled using the U of A record and the following regression relationship:

$$\mathbf{y = 0.9451x - 4.3646} \quad \mathbf{R^2 = 0.9251}$$

*where x = U of A max temperature*

For the period 1965-1981 gaps in the Oracle record were filled using the Sabino Canyon record and the following regression relationship:

$$\mathbf{y = 0.9359x - 3.5625} \quad \mathbf{R^2 = 0.9412}$$

*where x = Sabino Canyon max temperature*

The following gaps (days in year) existed in both the U of A and Oracle records prior to 1949 so were filled with linear interpolation between the two adjoining data points:

1893 69-72, 104-112, 119-122, 167-172, 227-232

1894 11-16, 29-36, 105-107, 177

1900 60

1911 318  
 1915 318-326  
 1920 276-280  
 1928 182-185  
 1936 279-280  
 1938 320

Gaps in Tucson Farm record:

For the period 1949-1982 gaps in the Tucson Farm record were filled using the Sabino Canyon record and the following regression relationship:

$$y = 0.9656x + 2.5678 \quad R^2 = 0.9796$$

where x = Sabino Canyon max temperature

For the period 1982-1999 gaps in the Tucson Farm record were filled using the U of A record and the following regression relationship:

$$y = 0.9728x + 1.9367 \quad R^2 = 0.9611$$

where x = U of A max temperature

*II.1.ii. Minimum Temperature*

(in °F , model converts to °C)

Actual data from Palisades: 1965-1981, includes gaps

Reconstructed data for Palisades: 1893-1964, 1982-1999, plus gaps in original record  
 Records and regression relationships used for various time periods:

Using average of U of A and Oracle averaged record:

**1893 - 1964 and 1982-1999 plus gaps in Palisades record between 1965-1981:**

$$y = 0.8503x - 7.1634 \quad R^2 = 0.8588$$

where x = Average of U of A and Oracle min temperature.

Gaps in the U of A record:

For the period 1893 - 1949 gaps in U of A record were filled using the Oracle record and the following regression relationship:

$$y = 0.9463x + 8.6709 \quad R^2 = 0.787$$

where x = Oracle min temperature.

For the period 1949 - 1999 gaps in U of A record filled using the Tucson Farm record and the following regression relationship:

$$y = 0.9032x + 10.814 \quad R^2 = 0.9238$$

where x = Tucson Farm min temperature.

The following gaps (days in year) existed in both the U of A and Oracle records, these were filled with linear interpolation between the two adjoining data points:

1893 69-72, 104-112, 119-122, 167-172, 227-232

1894 11-16, 32-39, 105-107, 177

1897 189  
 1900 60  
 1911 316  
 1912 186  
 1915 316-324  
 1920 274-278  
 1928 180-183  
 1929 347  
 1936 277-278  
 1975 105  
 1963 202

Gaps in the Oracle record:

For the period 1894 - 1999 gaps in Oracle record filled using the following regression relationship:

$$y = 0.8316x + 3.374 \quad R^2 = 0.787$$

where x = U of A min temperature.

*II.1.iii. Precipitation*

All precipitation reconstructions are based on regression equations forced through the origin. Winter (Jan-Apr, Nov-Dec) and Summer (May-Oct) periods were separated to facilitate better reconstructions.

Actual data from Palisades: 1965-1981, includes gaps

Reconstructed data for Palisades: 1895-1964, 1982-1999, plus gaps in original record.

Records and regression relationships used for various time periods:

**WINTER (Jan-Apr, Nov-Dec)**

Using average of U of A and Oracle averaged record:

**1895 - 1948:**  $y = 1.316166x$   $R^2 = 0.3963$   
 where x = U of A and Oracle average winter precipitation

Using Sabino Canyon record:

**1949 - 1964 and 1981 - 1982 and gaps in Palisades record:**  
 $y = 1.776523x$   $R^2 = 0.5909$   
 where x = Sabino Canyon winter precipitation

Using Cascabel record:

**1983 - 2000:**  $y = 2.4346x$   $R^2 = 0.591$   
 where x = Cascabel winter precipitation

Gaps in U of A record:

For the period 1895 - 1948 gaps in the U of A record were filled using the Oracle record and the following regression relationship:

$$y = 0.2667x \quad R^2 = 0.1448$$

where  $x$  = Oracle winter precipitation

For the period 1949 - 1999 gaps in the U of A record were filled using the Tucson Farm record and the following regression relationship:

$$y = 0.643x \quad R^2 = 0.3633$$

where  $x$  = Tucson Farm winter precipitation

Gaps in Oracle record:

For the period 1895 - 1999 gaps in the Oracle record were filled using the U of A record and the following regression relationship:

$$y = 0.691x \quad R^2 = 0.1282$$

where  $x$  = U of A winter precipitation

Gaps in Sabino Canyon record:

For the periods 1949 - 1964 and 1981 - 1982 gaps in the Sabino Canyon record were filled using the Tucson Farm record and the following regression relationship:

$$y = 0.9951x \quad R^2 = 0.7771$$

where  $x$  = Tucson Farm winter precipitation

**SUMMER (May - October)**

Using U of A and Oracle averaged record:

$$1895 - 1960: \quad y = 1.084108x \quad R^2 = 0.267$$

where  $x$  = U of A and Oracle average summer precipitation

Using U of A, Oracle, San Manuel, Kitt Peak and Tucson Airport averaged record:

1961 - 1964 and 1981 - 1999 and gaps in Palisades record:

$$y = 1.391374x \quad R^2 = 0.3609$$

where  $x$  = Average of U of A, Oracle, Kitt Peak, San Manuel, Tucson Airport.

Gaps in the U of A record:

For the period 1895 - 1948 gaps in the U of A record were filled using the Oracle record and the following regression relationship:

$$y = 0.2667x \quad R^2 = 0.1448$$

where  $x$  = Oracle summer precipitation

For the period 1949 - 1999 gaps in the U of A record were filled using the Tucson Farm record and the following regression relationship:

$$y = 0.643x \quad R^2 = 0.3633$$

where  $x$  = Tucson Farm summer precipitation

Gaps in the Oracle record:

For the period 1895 - 1999 gaps in the Oracle record were filled using the U of A record and the following regression relationship:

$$y = 0.691x \quad R^2 = 0.1282$$

where  $x$  = U of A summer precipitation

Gaps in the Kitt Peak record:

For the period 1961 - 1999 gaps in the Kitt Peak record were filled using the Tucson Farm record and the following regression relationship:

$$y = 0.8306x \quad R^2 = 0.142$$

where x = Tucson Farm summer precipitation

Gaps in the San Manuel record:

For the period 1955 - 1999 gaps in the San Manuel record were filled using the Tucson Farm record and the following regression relationship:

$$y = 0.5184x \quad R^2 = 0.2066$$

where x = Tucson Farm summer precipitation

Gaps in the Tucson Airport record:

For the period 1948 - 1999 gaps in the Tucson Airport record were filled using the U of A record and the following regression relationship:

$$y = 0.5926x \quad R^2 = 0.3654$$

where x = U of A summer precipitation

*II.1.iv. Dew Point Temperature*

(in °C)

Actual data from Palisades: 1<sup>st</sup> April 1997 - 31<sup>st</sup> Dec 1997, includes gaps

Reconstructed data for Palisades: 1<sup>st</sup> October 1948 - 30<sup>th</sup> June 1998, plus gaps in original record.

Records and regression relationships used for various time periods:

Using Tucson Airport record:

**1948 - 1964 and 1984 - 1998:**

$$y = 0.8836x - 5.9552 \quad R^2 = 0.7952$$

where x = Dew point temperature (°C) at Tucson Airport

Gaps in the Tucson Airport record:

For the period 1965 - 1983 gaps in the Tucson Airport record were filled using the Tucson Airport 700hPa upper air record and the following regression relationship:

$$y = 0.0742x + 4.2468 \quad R^2 = 0.617$$

where, x = Dew point temperature at 700hPa (°F) at Tucson Airport  
**note:** y = Reconstructed Tucson Airport dew point temperature in °C

Other gaps in the Tucson Airport record:

For the period 1948 - 1998 remaining gaps in the Tucson Airport record were filled by linear interpolation between the two adjoining data points.

## II.2. Isotope Inputs

### II.2.i. $\delta^{13}\text{C}$ of atmospheric $\text{CO}_2$

Annual values of atmospheric  $\delta^{13}\text{C}$  are estimated from ice core and flask measurements (figure II.1). The values are changed on January 1<sup>st</sup> each year. No allowance is presently made for intra-annual changes in  $\text{CO}_2$ .

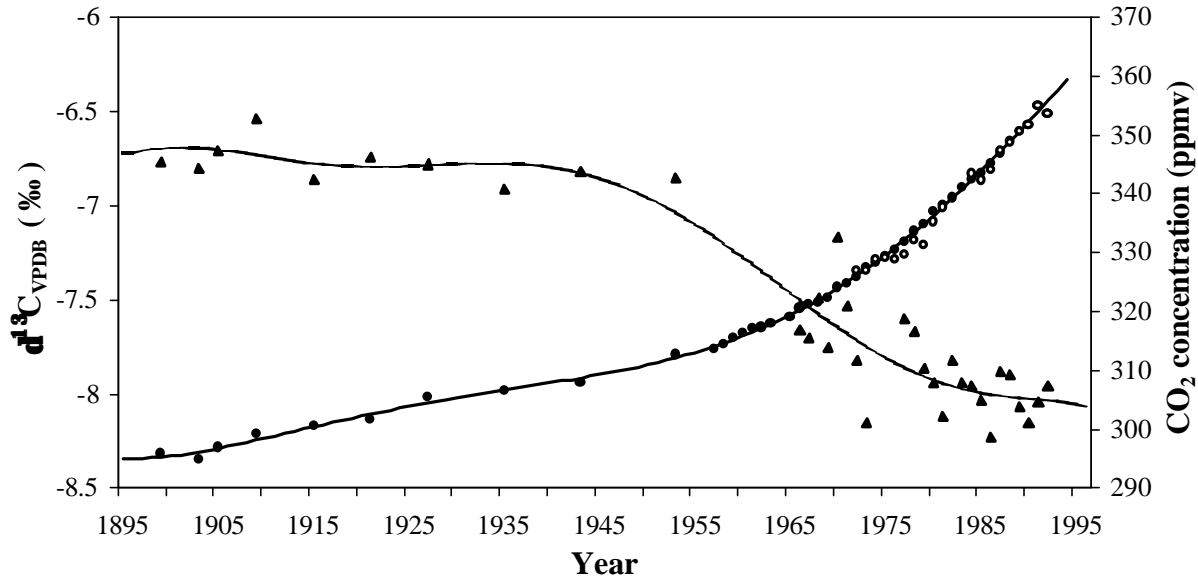


**Figure II.1.** Atmospheric  $\text{CO}_2$  concentration (circles) and carbon isotope ( $\delta^{13}\text{C}$ ) composition (triangles).  $\text{CO}_2$  concentration data is from the Siple ice-core, Antarctica; filled circles, 1899 - 1953 (Friedli et al., 1986), South Pole summer average (April - September) air flask measurements; filled circles, 1957 - 1988 (Keeling and Whorf, 1996) and Schauinsland, Germany summer average air flask measurements; open circles 1972 - 1992.  $\delta^{13}\text{C}$  data is from the Siple ice core; filled triangles, 1895 - 1953 (Friedli et al., 1986), Vermont, Austria summer average (April - September) air flask measurements; filled triangles, 1966 - 1974 (Levin et al., 1994), Schauinsland summer average air flask measurements and filled triangles, 1977 - 1992 (Levin et al., 1994). A 6<sup>th</sup> order polynomial fitted to the  $\delta^{13}\text{C}$  data (excluding the eastern England measurements) is assumed to be the general atmospheric  $\delta^{13}\text{C}$  trend over the last 100 years.

### II.2.ii. $\delta^{18}\text{O}$ and $\delta\text{D}$ of precipitation and atmospheric water vapor

Measurements of the  $\delta^{18}\text{O}$  and  $\delta\text{D}$  of precipitation collected at a site in Tucson from January 1982 (Long, unpublished data) are used as initial inputs for the soil water model. The following methods are used to fill gaps that exist in these records. Where values are not available, but a precipitation event has occurred at the site, a regression model between  $\delta^{18}\text{O}$  of precipitation and average daily temperature for the same site in Tucson is used to estimate  $\delta^{18}\text{O}$  of precipitation (figure II.2).

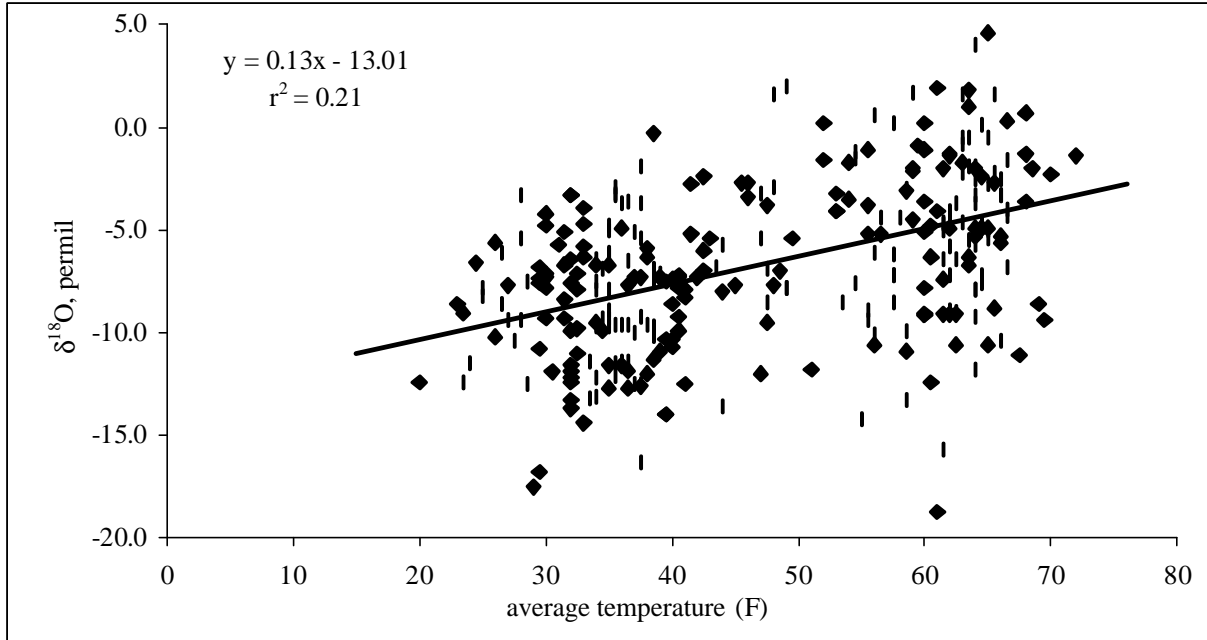


**Figure II.2.** Regression model used to fill gaps in  $\delta^{18}\text{O}$  of precipitation data

Where the  $\delta^{18}\text{O}$  of atmospheric vapor is not available it is estimated from a regression model ( $\delta^{18}\text{O}_{\text{vap}}(i) = (0.4002 * \delta^{18}\text{O}_{\text{prec}}(i)) - 13.627$ ) between  $\delta^{18}\text{O}$  of atmospheric vapor and  $\delta^{18}\text{O}$  of precipitation (figure II.3).

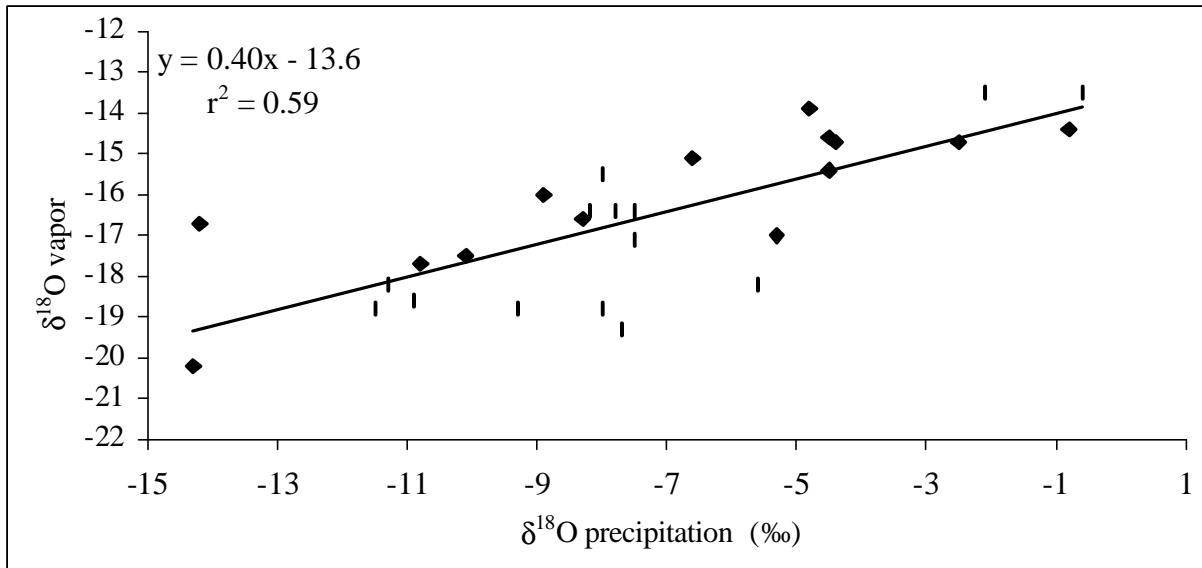


**Figure II.3.** Regression relationship of  $\delta^{18}\text{O}$  of vapor and  $\delta^{18}\text{O}$  of precipitation at Tucson. Regression model is used to fill gaps in the  $\delta^{18}\text{O}$  of vapor series.

Where data is not available the  $\delta\text{D}$  of precipitation and vapor was calculated from a regression model between  $\delta^{18}\text{O}$  of precipitation/vapor and  $\delta\text{D}$  of precipitation/vapor (figure II.4).

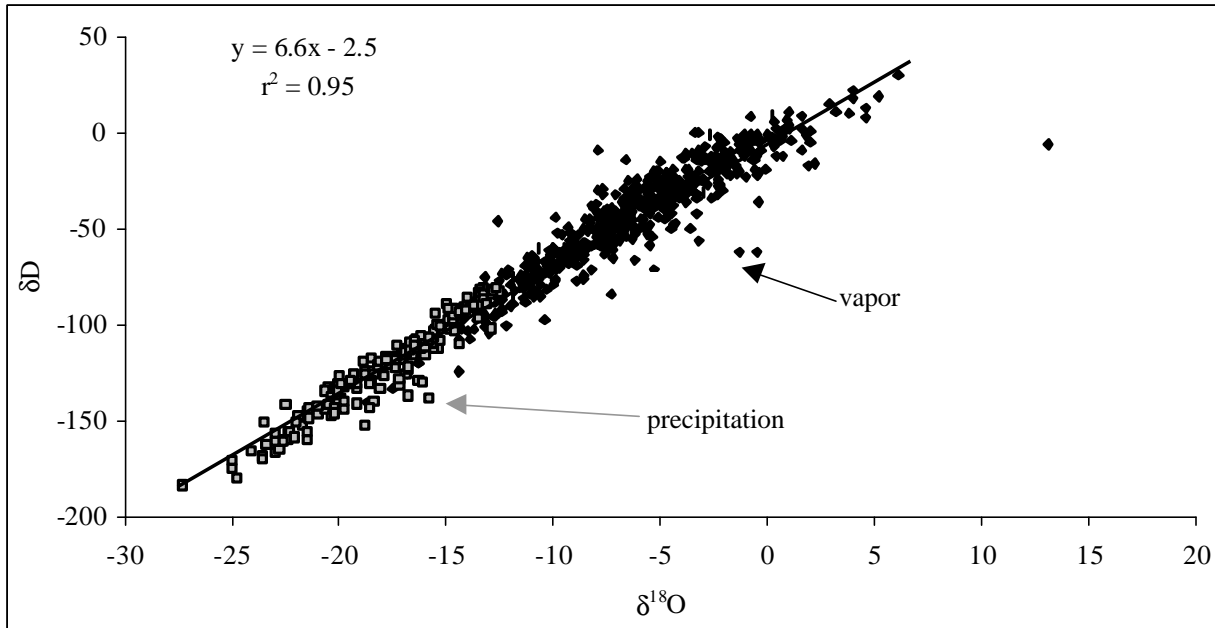


**Figure II.4.** Regression relationship of  $\delta^{18}\text{O}$  and  $\delta\text{D}$  (versus VSMOW) in precipitation at Tucson, Arizona, USA. This regression model is used to fill gaps in the  $\delta\text{D}$  of precipitation and vapor series.

### II.3. Allometric Data

#### II.3.i. Tree age:height:radius curve

The existing TreeRing model (Fritts *et al*, 1999) assumed that height growth, crown growth, root growth and soil volume were constants. However in applications to younger trees it was necessary to simulate the yearly increase in height, crown, stem, roots and soil volume for the growing tree. We therefore collected field measurements of tree diameter at breast height (dbh is 1.3 m) and tree height from 21 trees in the study area. In addition, we examined the existing cores from these trees and recorded the pith year (dbh), the first year in which the cell size and wall thickness measurements began, the distance in mm between them, heartwood width and sapwood width. Some cores did not reach the pith so in these cases a template of concentric circles was used to estimate the number of years and distance to the center using the curvature of the innermost rings in the core.

These measurements were entered into a Microsoft Excel spreadsheet and equations were developed for estimating the heartwood radius from the total radius of the stem and total tree height from the age of the tree (Figures II.5 and II.6).

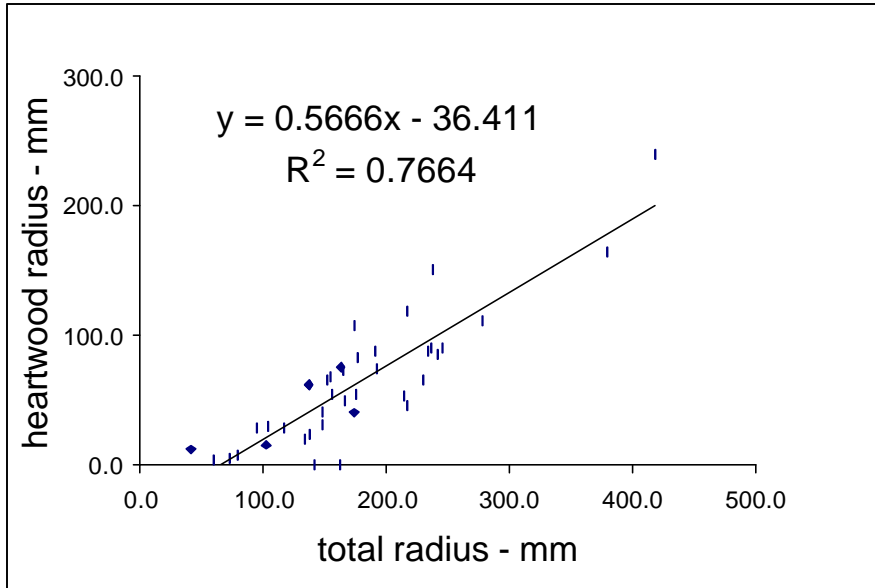


**Figure II.5.** The equation used to estimate heartwood radius from the total radius of the tree stem derived from observations on the study area trees.

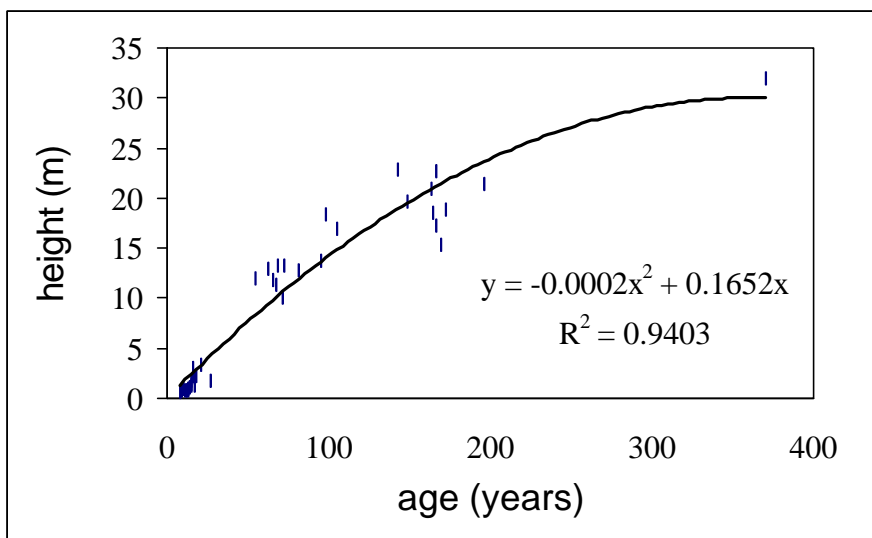


**Figure II.6.** The equation used to estimate height from tree age derived from observations on the study area trees.

The necessary data to estimate stem height growth, crown mass and other related parameters were entered into file Trg70.i0. The subroutine *Trginput.for* was rewritten to read these data and to calculate the following:

1. The age and radius ( $r_t$ ) of the ring prior to the beginning of existing independent measurements were calculated from the pith date and radius measurement. If the simulation did not begin with the first available measurement, the measurement file with a .CRN extent is opened, and the ring width measurements are read from this file up to the starting date of the simulation.
2. A young tree was harvested and the needle traces were used to determine the number of needles produced in each internode year from 1962 to 1998 and the length of the internode was measured (Hemming *et al.* 2001). The number of needles formed each year was converted to an index by dividing each number by the average. A multiple regression estimated the needle number index from monthly temperature and precipitation of current and prior year. The coefficients from the regression were entered as parameter zini(51-99) (Table 4) with all zero coefficients entered as blank fields. Subroutine TRGINPUT.FOR calculates the estimated needle number index using the monthly climatic data from the current and previous year. During the first year where the prior year climatic information is not available the index is assigned a value of 1.0
3. Stem area at breast height is then calculated from the current radius.
4. The maximum depth and area of the soil are read from p(14) and p(15). However, zini(37) is a Michaelis-Menten constant age\*. If its value is greater than zero, depth is calculated as a function of age:  $depth_t = age / (age + age^*) * p(14)$ . The soil area is estimated later as a fractional percent of crown area (zini(29)) if zini(29) is greater than zero.
5. Height (h) is calculated as a function of age using zini(18) and zini(19):  $h = -0.0002 \text{ age}^2 + 0.1605 \text{ age}$  (Fig. 6). The maximum height is calculated from the maximum age using the same parameters
6. The surface (s) of the cambium in the stem and root is estimated from the surface of an open-top cylinder as  $s = 2 \pi * \text{radius} * (\text{tree height} + \text{depth of roots})$ .
7. Heartwood radius is estimated from the total radius as observed on cores extracted from the study site trees:  $r_h = 0.5666r_t - 36.411$ . If the estimated  $r_h$  is less than 0,  $r_h$  is set to zero (figure II.5). The heartwood area in  $\text{cm}^2$  and  $\text{m}^2$  is then calculated.
8. Sapwood radius ( $\Delta$ ) and area are calculated by subtracting the heartwood radius.
9. The crown mass for *Pinus ponderosa* is calculated from the sapwood area and product of crown ratio and crown length using the allometric equations of Monserud & Marshall (1999). The crown ratio and length were measured from the study area trees.
10. Crown area is estimated as a function of crown mass by multiplication of the mass with p(3), the coefficient of conversion of leaf mass to area. This parameter is obtained using fresh 5-needle clusters sampled from the study area trees. Area is estimated from the length and width of the fresh needles and divided by their dry weight.

11. The soil area available to precipitation is estimated as a fractional percent of crown area (zini(29)).
12. The phloem area and volume are estimated as a cylinder surrounding the stem volume estimate using phloem thickness (zini(13)) obtained from the study area trees.
13. The circumference of the cambium and the number of tracheid initials are estimated from the tangential size of the initials (pp(28)) and the fractional percent of rays (zini(24)). Cambial area (S) is the surface of the estimated cylinder surrounding the stem.
14. The volume of coarse roots is estimated from the stem area at the soil surface and depth of roots. The density of root wood is assumed to be the same as density of stem wood (den(3)).
15. A special set of coefficients is calculated for use in the estimation of respiration. Coefficients K, Sapwood volume (V) and N are calculated as:  $K = \frac{\Delta}{(1-\Delta)/2/r_t}$ ,  $V = K*S$  and  $N = 2*\pi*r_t$ , where  $\Delta$  is the sapwood radius,  $r_t$  is the radius of the stem wood and S is the surface area of the cambium.
16. Sapwood mass is calculated from sapwood  $V*den(2)$  and phloem mass from phloem volume\*den(2).
17. Fine root mass is estimated as a proportion of the other masses:  $R_{mass} = zini(39)*crown\ mass*sapwood\ mass*phloem\ mass$ .
18. In the first year the mass of the current and previous summer foliage is calculated as  $\frac{1}{2}$  of the total mass. In subsequent years the mass of the second year needles is subtracted from the total foliage mass to obtain the current year's needle mass.
19. The current year uncorrected needle mass is multiplied by the needle index to account for the effects of climate on needle growth.

Subroutine TRGINPUT.FOR is called once at the beginning of the first year to calculate the initial value of these variables and then again on day p(51) to calculate the needle growth of the current year and all other input variables. It is then called on day p(51) in each subsequent year.

In normal mode, when op(20) is zero, these calls on day p(51) use the dendrograph estimate of growth in the current year to estimate the new stem radius and all the calculations are made using this datum. However, in the subsequent year the true estimated ring width of the previous year replaces this estimate and the current growth, estimated from the dendrograph estimate, is added to estimate the stem radius.

There is a second mode, when op(20) is 1, in which the calls on day p(51) use the actual ring widths rather than the estimated value. This allows the model to track any anomalous growth patterns in the simulated tree. This option has not been used extensively and is not well tested at present. Normal mode is used in subsequent discussions.

The array, hold, passes the following values to the main program:

1. Hold(1): Current radius m
2. Hold(2): Empty
3. Hold(3): Empty
4. Hold(4): Sapwood mass kg

5. Hold(5): Fine root mass kg
6. Hold(6): Height in m
7. Hold(7): Not used
8. Hold(8): Sapwood Volume (V)
9. Hold(9): K which becomes variable form in the main program.
10. Hold(10): Volume of living stem cells
11. Hold(11): Mass of 1-year-old needles kg
12. Hold(11): Mass of 2-year-old needles kg
13. Hold(12-20) Needle mass for trees holding up to 10-year-old needles.

A total of 29 input variables are written to file “\*I.DAT” along with the contents of the arrays “Hold” and “Zini” from Trg70.i0.

*II.3.ii. Relationship between volume and mass of sapwood and the volume of live cells in the sapwood.*

The sapwood volume, V, is:

$$(1) \quad V = \pi\Delta(2R - \Delta)h$$

The sapwood surface area, S, is:

$$(2) \quad S = 2\pi Rh$$

The relationship between the sapwood volume and the surface area is:

$$(3) \quad V = \Delta(1 - \Delta/2R)S,$$

$$\text{or} \quad V = kS,$$

where,  $k = \Delta(1 - \Delta/2R)$ .

The number of cellular files, N, is calculated as:

$$(4) \quad N = 2\pi R/d_{\text{tang}},$$

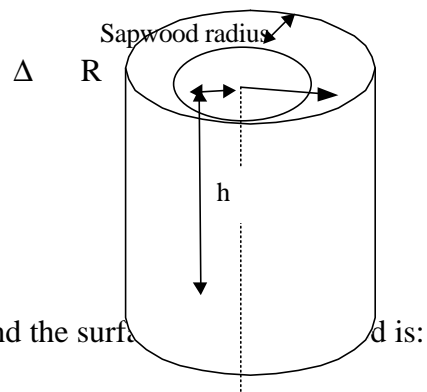
where,  $d_{\text{tang}}$  is the tangential cell size of the initial cell.

If cell wall area is denoted by  $a$  then the cell wall volume,  $V_w$ , of for “long” cells (where length is equal the height,  $h$ , of the tree) is:

$$(5) \quad V_w = ahN$$

or by rewriting equations 2 and 3:

$$(6) \quad V_w = ah2\pi R/d_{\text{tang}} = a/d_{\text{tang}}S = a/d_{\text{tang}} V/k$$



Equation 6 is used for calculation of the cell wall mass dynamic. Cell wall mass is:

$$(7) \quad M = V_w \rho$$

where,  $\rho$  is the density of wall in mMCO<sub>2</sub>/m<sup>3</sup>.

The density of wall is assumed to be 1300 kg/m<sup>3</sup> or 1.3<sup>-12</sup> g/micron<sup>3</sup> (Silkin, 2001). Assimilated CO<sub>2</sub> is converted to dry matter equivalents by multiplying by 28.5 g mol<sup>-1</sup> (Landsber, 1986 p89). Dry weight is then converted to mMCO<sub>2</sub> units by multiplying by 1/28.5=35.09 mMCO<sub>2</sub> g<sup>-1</sup>. Therefore, for additional cell wall area and volume growth we used the coefficient 45.617 mMCO<sub>2</sub>/micron<sup>3</sup> (1.3<sup>-12</sup> x 35.09).

## II.4. Parameters

**Table 1.** Filename 'TRG70.PAR', parameters (p) for main TreeRing program (TRG70.FOR)

2.0	1		Maximum age of foliage	yr
20.0	2	halfRad	Radiation at which photosynthesis reaches 1/2 maximum	Wm <sup>-2</sup>
7.0	3		Coefficient of conversion of leaf mass to area	m <sup>2</sup> kg <sup>-1</sup>
250.0	4	Rmin	Minimum resistance to diffusion of water	sm <sup>-1</sup>
550.0	5	Rmax	Maximum resistance to diffusion of water	sm <sup>-1</sup> 100 <sup>-1</sup>
	6			
-5.0	7	Ct	Period for averaging leaf growth for threshold rate	Days
0.01	8	Cts	Critical threshold average rate to stop crown growth	
0.01	9	sm1	Wilting point	vv <sup>-1</sup>
0.109	10	sm2	Optimal soil moisture	vv <sup>-1</sup>
0.23	11	sm3	Maximum optimal soil moisture	vv <sup>-1</sup>
0.25	12	sm4	Maximum moisture at which water absorption stops	vv <sup>-1</sup>
0.24	13	sm5	Field capacity	vv <sup>-1</sup>
0.6754	14	h	Maximum depth of the tree root system	m
30.0	15	Sarea	Maximum soil surface area, actual estimated from age or height	m <sup>2</sup>
0.89	16	K6	Coefficient of available precipitation	lDay <sup>-1</sup>
100.0	17	AP	Maximum available precipitation	mm
0.5216	18	K1	Water absorption per unit of root	kgdm <sup>-3</sup> h <sup>-1</sup>
1.65	19	K3	Coefficient for diffusion of CO <sub>2</sub> relative to water	
0.45	20		Carbon concentration of wood	kgC <sup>-1</sup> kg dry wt <sup>-1</sup>
-10.0	21	Tmin	Minimum day temperature for photosynthesis	Celsius
9.57	22	Topt1	Optimal temperature for photosynthesis	Celsius
23.0	23	Topt2	Maximum optimal temperature for net photosynthesis	Celsius
40.0	24	Tmax	Tmax - Maximum temp when net photosyn. becomes 0	Celsius
12.5	25	CO2a	CO <sub>2</sub> concentration in the air	mMm <sup>-3</sup>
1.5	26	A	Minimum CO <sub>2</sub> i (photosynthetic compensation point)	mMm <sup>-3</sup>
10.5	27	B	Maximum (saturation) concentration of CO <sub>2</sub> i	mMm <sup>-3</sup>
0.419	28	CT	Relative crown growth rate threshold to form latewood	
0.38	29	Ctm	Crown growth threshold to begin cell wall thickening	
120.0	30		Maximum average resistance to prevent growth beginning	
20.0	31		Period to calculate temperature sum	Days
120.0	32	sumt	Temperature sum to begin growth	Celsius
0.0	33		Days after Critical Day Length that growth can begin 0.0	Days
10.0	34		Michaelis-Menthon coefficient of maintenance respiration	
-5.7	35	astmin	Minimum temperature for leaves	Celsius
10.1	36	astopt1	Optimal temperature for leaves	Celsius
22.1	37	astopt2	Maximum optimal temperature for leaves	Celsius
30.1	38	astmax	Maximum temperature where leaf growth becomes 0	Celsius
	39			

0.0	40	r1	Diffusion of water from soil below field capacity	
0.072	41		Minimum water concentration in the stem	$\text{vV}^{-1}$
0.72	42		Maximum water concentration in the stem	$\text{vV}^{-1}$
2.0	43		Hourly rate of water absorption from stem	$\text{kgdm}^{-3}\text{h}^{-1}$
0.08	44		Hourly rate of stem water recharge from soil	$\text{kgdm}^{-3}\text{h}^{-1}$
1.0	45		Scale for active radius	
	46			
11.0	47		Sensitivity of leaf growth to resistance: full(10), low (1)	
10.0	48		Sensitivity of root growth to resistance: full(10), low (1)	
0.555	49		Fractional percent leaf surface exposed to light	
12.5	50		Day length to begin growth	Hours
244.0	51		Day number to calculate new needle mass	Day
28.0	52		Number of days of transition to new needle mass	Days
	53			
	54			
	55			
0.03	56	Pmax	Maximum rate of photosynthesis	$\text{mMm}^{-2}\text{s}^{-1}$
0.0	57			
4.0	58		Difference needed to begin averaging for earlywood-latewood	
188.0	59		Day number to begin checking for earlywood-latewood boundary	
4.0	60		Number of days to average for earlywood-latewood boundary	
	<b>Density parameters</b>			
1200.0	1	den(1)	Density of xylem cell wall	$\text{kgm}^{-3}$
360.0	2	den(2)	Density of phloem, rays (balsa wood)	$\text{kgm}^{-3}$
459.0	3	den(3)	Density of Ponderosa pine wood (Carey et al, 1966)	$\text{kgm}^{-3}$
	4			
	5			
	<b>Maintenance respiration</b>			
180.0	1	rnc(1)	Coefficient for foliage @t=10°C (Ryan, 1995)	$\text{mMCO}_2\text{m}^{-3}\text{day}^{-1}$
100.0	2	rnc(2)	Coefficient for living stem tissues @t=10°C (Ryan, 1995)	$\text{mMCO}_2\text{m}^{-3}\text{day}^{-1}$
160.0	3	rnc(3)	Coefficient for roots @t=15°C (Ryan, 1995)	$\text{mMCO}_2\text{m}^{-3}\text{day}^{-1}$
0.069	1	rnt(1)	Temperature coefficient for foliage	1/0 deg.C
0.069	2	rnt(2)	Temperature coefficient for living stem tissues	1/0 deg.C
0.069	3	rnt(3)	Temperature coefficient for roots	1/0 deg.C
	<b>Carbon use efficiency in growth respiration of...</b>			
0.785	1	grc(1)	Leaves/crown	$\text{mMCO}_2\text{kg}^{-1}\text{day}^{-1}$
	2	grc(2)		
	3	grc(3)		
	4	grc(4)		
0.8	5	grc(5)	Roots	$\text{mMCO}_2\text{kg}^{-1}\text{day}^{-1}$
	<b>Coefficients in Michaelis Menton equation for concentration of sucrose when 1/2 maximum rate</b>			
15000.0	1	gc(1)	Michaelis Menton constant for leaves when 1/2 maximum rate	mM
1000.0	2	gc(2)	Concentration of sucrose when leaf growth stops	mM
	3	gc(3)		
525.0	4	gc(4)	Concentration of sucrose when root growth stops	mM

798.5	5	gc(5)	Michaelis Menton constant for roots when 1/2 maximum rate	mM
<b>Proportion of growing tissue of living mass in...</b>				
0.012	1	prp(2)	Leaves	
0.0	2	prp(1)	Cambial area, calculated by TRGINPUT program if 0	
0.023	3	prp(3)	Roots	
<b>Maximum growth rate of...</b>				
1.67	1	upt(1)	Leaves (increase to shorten season)	1/day
0.0494	2	upt(2)	Roots	
0.0	3	upt(3)		
0.0	4	upt(4)		
0.0	5	upt(5)		
<b>Beginning threshold for Resistance Limitation to begin (250 Min)</b>				
40000.0	1	xrmn(1)	Leaves	
40000.0	2	xrmn(2)	Roots	
	3	xrmn(3)		
	4	xrmn(4)		
	5	xrmn(5)		
<b>Max Resistance when growth stops (55000 Max)</b>				
55000.0	1	xrmx(1)	Leaves	
55000.0	2	xrmx(2)	Roots	
	3	xrmx(3)		
	4	xrmx(4)		
	5	xrmx(5)		

**Table 2.** Filename 'CAMB70.PAR', parameters (b) for CAMBIUM subroutine (camb70.for)

16.3	1		Minimum cell size		
49.0	2		Maximum cell size		
30.0	3		Tangential cell size		
2.0	4		Minimum cell wall thickness		
15.0	5	Amax	Maximum cell wall area		
0.18	6		Minimum of lumen area (fractional percent)		
2.0	7		Minimum cell wall thickness		
	8				
	9				
7.9	10		Size of dividing cell between G1 & S (Chromosomes begin to replicate)		
9.0	11		Size of dividing cell between S & G2 (Division begins)		
9.5	12		Size dividing cell between G2 & M (Mitosis begins)		
10.0	13		Size of dividing cell when it begins to divide		
	14				
	15				
	16				
	17				
	18				
	19				
50.0	20		Maximum number of cells in any cambial zone		
		<b>Control of cambial division</b>			
0.01	21		Minimum growth rate below which the cambium is dormant		
0.32	22		Scalar of growth rate		
0.16	23		Growth rate during S, G2 and M phases of the cell cycle		
0.225586	24	Kmax	Maximum slope of division rate		
10.0398	25	Vp	Division rate at 60mKm assumed when few cells present		
0.06	26		Coefficient b3 (Vmin) equation 6.5. Curve to switch to enlargement		
32.55	27		b2(Vmin) equation 6.5. Switch to enl. curve (Increase to incr. enl. time)		
17.3281	28		Distance of growing cells when slope of division rate is 1/2 maximum	microns	
12.4	29		Day length to stop cambial and leaf growth	hours	
-10.0	30		Period to average Ct		
1.0752	31		Sensitivity of division to Ct (1 is minimum - 10 is maximum)		
5.5	32		Sensitivity of vmin in Cambium to Ct (1 is maximum - 10 is minimum)		
20400.0	33		Minimum sugar concentration when division stops	mK	
235430.0	34		Michaelis Menton coefficient for sugar limitation to division	mK	
10000.0	35		Maximum resistance for division to occur, division stops <55000		
400.0	36		Minimum resistance to division limitation, limitation begins >250		
-5.0	37		Minimum temperature for division		
10.0	38		Optimal temperature for division		
23.0	39		Maximum optimal temperature for division		
40.0	40		Maximum temperature where division becomes 0		
10.0	41		Sensitivity of division to resistance (10 is maximum - 1 is minimum)		
		<b>Control of enlargement</b>			
0.1	42	Vcre	Critical rate when enlargement switches to maturation	micronsDay <sup>-1</sup>	
	43				

0.0169	44	Potential from distance	
9.5	45	Minimum distance	
0.4	46	Rate of enlargement	micronsDay <sup>-1</sup>
	47		
	48		
4.0	49	Sensitivity of enlargement to resistance (10 is maximum - 1 is minimum)	
-5.0	50	Period of average for control of enlargement	Days
2.0	51	Sensitivity of enlargement to Ct (10 is maximum - 1 is minimum)	
	52		
40000.0	53	Minimum sugar concentration when enlargement stops	mK
22900.0	54	Michaelis Menton coefficient in equation of growth control by sucrose	mK
55000.0	55	Maximum resistance for enlargement to occur, enlargement stops <55000	
350.0	56	Minimum resistance to enlargement limitation, limitation begins >250	
-5.0	57	Minimum temperature for enlargement to occur	°C
7.0	58	Optimal temperature for enlargement rate	°C
25.5	59	Maximum optimal temperature for enlargement rate	°C
30.0	60	Maximum temperature where enlargement becomes	°C
		<b>Control of maturation</b>	
	61		
0.0	62	V <sub>crm</sub> Critical rate to stop thickening	mKmDay <sup>-1</sup>
0.2	63	Cell size control of thickening rate	
0.2	64	Rate of thickening	
	65		
	66		
	67		
	68		
10.0	69	Sensitivity of maturation to resistance (10 is maximum - 1 is minimum)	
-2.0	70	Period of average for control of maturation	Days
10.0	71	Sensitivity of maturation to C <sub>tm</sub> (10 is maximum - 1 is minimum)	
	72		
30000.0	73	Minimum sugar concentration when maturation stops	mK
23437.5	74	Michaelis Menton coefficient in equation of control growth by sucrose	
10000.0	75	Maximum resistance for maturation to occur, maturation stops <55000	
2050.0	76	Minimum resistance for maturation to occur, limitation begins >R <sub>min</sub>	
-5.0	77	Minimum temperature for wall thickening	°C
14.0	78	First optimal temperature for wall thickening	°C
28.5	79	Second optimal temperature for wall thickening	°C
35.0	80	Maximum temperature for wall thickening	°C
		<b>Control of respiration</b>	
25.0	81	Coefficient of maintenance respiration for stem cells b1	
0.0868	82	Temperature coefficient of maintenance respiration	
	83	R10, respiration at 10°C	
	84		
	85		
	86		
	87		
	88		
	89		

0.8	90	Efficiency of division growth	$\text{mMCO}_2\text{cell}^{-1}\text{day}^{-1}$
0.8	91	Efficiency of enlargement growth	$\text{mMCO}_2\text{cell}^{-1}\text{day}^{-1}$
0.8	92	Efficiency of maturation growth	$\text{mMCO}_2\text{cell}^{-1}\text{day}^{-1}$
	93		
	94		
	95		
	96		
	97		
	98		
	99		
0.0	100	Use only living cells for distance (0), Use all cells for distance (1)	

**Table 3.** Filename 'ISO.PAR', for ISOTOPE subroutine (isotope.for).

<b>Common parameters for isotope calculations (isoAll(i))</b>			
0.7	1	Leaf surface vapor pressure (vp) as proportion of external - internal vp's	
22.4	2	Volume of one mole of an ideal gas at STP ( T=0°C and P=101300Pa)	
273.15	3	Zero degrees Kelvin	°K
1.0	4	Portion of sucrose allocated to storage each day, 0.0=0%, 1.0=100%	
1.0	5	Maintenance respiration before growth in leaf? 1.0=yes, 2.0=no	
1.0	6	Maintenance respiration before growth in stem? 1.0=yes, 2.0=no	
1.0	7	Maintenance respiration before growth in root? 1.0=yes, 2.0=no	
	8		
	9		
	10		
	11		
	12		
	13		
	14		
	15		
<b>Carbon isotope parameters (isoC(i))</b>			
-4.4	1	Maximum fractionation from diffusion of CO <sub>2</sub> into leaf	
-30	2	Maximum fractionation from carboxylation	
3	3	Discrimination against <sup>13</sup> C during photorespiration	
1.5	4	Discrimination against <sup>13</sup> C during dark respiration	
10	5	Difference in altitude between trees and met. station (minus=met lower)	m
	6		
148	7	CO <sub>2</sub> compensation point	mMCO <sub>2</sub>
0.245	8	Carboxylation efficiency (k in the Farquhar equation)	
	9		
	10		
	11		
	12		
	13		
	14		
	15		
<b>Oxygen isotope parameters (isoO(i))</b>			
	1		
1	2	Proportion of Craig-Gordon leaf water in bulk leaf water	
0.12	3	Proportion of carbon-bound oxygen in cellulose from xylem water	
1.137	4	Majoube (1971) water-vapor 'a' term in equation of T V <sub>s</sub> <sup>18</sup> O <sub>l-v</sub>	
-0.4156	5	Majoube (1971) water-vapor 'b' term in equation of T V <sub>s</sub> <sup>18</sup> O <sub>l-v</sub>	
-2.0667	6	Majoube (1971) water-vapor 'c' term in equation of T V <sub>s</sub> <sup>18</sup> O <sub>l-v</sub>	
0.002005	7	<sup>18</sup> O: <sup>16</sup> O for reference material - VSMOW	
1.0285	8	Craig-Gordon model kinetic diffusion (k <sub>d</sub> ) fractionation into stomatal pore (Merlivat 1978)	
1.0189	9	Craig-Gordon model, k <sub>d</sub> fractionation in boundary layer (Flanagan & Ehleringer 1991)	
27	10	Biochemical fractionation during carbohydrate synthesis	

0.1351	11	Regression slope coefficient for average daily temperature to $\delta^{18}\text{O}$ precipitation relationship	
-13.028	12	Regression intercept for average daily temperature to $\delta^{18}\text{O}$ precipitation relationship	
-3.28	13	$\delta^{18}\text{O}$ altitude effect from UofA to Palisades (1640m alt difference)	
0.4002	14	Regression slope coefficient for $\delta^{18}\text{O}$ precip. to $\delta^{18}\text{O}$ vapor relationship	
-13.627	15	Regression intercept for $\delta^{18}\text{O}$ precip. to $\delta^{18}\text{O}$ vapor relationship	
		<b>Hydrogen isotope parameters (isoH(i))</b>	
	1		
1	2	Proportion of Craig-Gordon leaf water in bulk leaf water	
0.42	3	Proportion of carbon-bound hydrogen in cellulose from xylem water	
24.844	4	Majoube (1971) water-vapor 'a' term in equation of T Vs DI-v	
-76.248	5	Majoube (1971) water-vapor 'b' term in equation of T Vs DI-v	
52.612	6	Majoube (1971) water-vapor 'c' term in equation of T Vs DI-v	
0.000156	7	D:H for reference material - VSMOW	
1.025	8	Craig-Gordon model, $k_d$ fractionation through stomatal pore (Merlivat 1978)	
1.017	9	Craig-Gordon model, $k_d$ fractionation in boundary layer (Flanagan & Ehleringer 1991)	
-171	10	Autotrophic biochemical fractionation during carbohydrate synthesis (Yakir & DeNiro 1990)	
158	11	Heterotrophic biochemical fractionation during carbohydrate synthesis (Yakir & DeNiro 1990)	
6.6149	12	Regression slope coefficient for $\delta^{18}\text{O}$ precip to $\delta\text{D}$ precip and vapor relationship	
-2.4751	13	Regression intercept for $\delta^{18}\text{O}$ precip to $\delta\text{D}$ precip and vapor relationship	
	14		
	15		

**Table 4.** Filename 'TRG70.IO', initial input parameters.

Initial input parameters, zini(i)			
0.0	1	Initial stem water	
	2		
	3		
-15.0	4dDstL	Hydrogn isotope composition ( $\delta D$ ) of initial starch in the leaves	‰VSMOW
-15.0	5dDstS	$\delta D$ of initial starch in the stem	‰VSMOW
-15.0	6dDstR	$\delta D$ of initial starch in the roots	‰VSMOW
35.0	7d18stL	Oxygen isotope composition ( $\delta^{18}O$ ) of initial starch in the leaves	‰VSMOW
35.0	8d18stS	$\delta^{18}O$ of initial starch in the stem	‰VSMOW
35.0	9d18stR	$\delta^{18}O$ of initial starch in the roots	‰VSMOW
-22.0	10d13CstL	Carbon isotope composition ( $\delta^{13}C$ ) of initial starch in the leaves	‰VPDB
-22.0	11d13CstS	$\delta^{13}C$ of initial starch in the stem	‰VPDB
-22.0	12d13CstR	$\delta^{13}C$ of initial starch in the roots	‰VPDB
0.0	13	Thickness of phloem	m
0.2	14	Initial soil moisture	$v v^{-1}$
2500.0	15	Initial photosynthate in the crown	mM
20000.0	16	Initial photosynthate in the stem	mM
2000.0	17	Initial photosynthate in the root	mM
-0.0002	18	Height equation coefficient for age <sup>2</sup>	m
0.1605	19	Height equation coefficient for age	m
0.5666	20	Heartwood area coefficient for age <sup>2</sup>	cm <sup>2</sup>
-36.411	21	Heartwood area coefficient for age	cm <sup>2</sup>
	22		
	23		
0.1	24	Fractional % rays / unit length of cambium	mm <sup>-1</sup>
0.0207	25	B0 Coefficient (from Monserud and Marshall, 1999)	
0.6903	26	B1 Exponent sapwood area / crown mass	cm <sup>2</sup> kg <sup>-1</sup>
0.9543	27	B4 Exponent crown length	m
0.44	28	Fractional % crown height / total tree height	mm <sup>-1</sup>
0.4	29	Fractional % soil surface area / leaf area	m <sup>2</sup> m <sup>-2</sup>
1919	30	Pith Date	y
1940	31	First measured year date	y
0.032	32	Distance from first measured year to pith	m
	33		
	34		
	35		
	36		
40	37	Age at which depth will be 50% of maximum depth	
0.00015	38	Average radial diameter of cambial cells	m
0.03	39	Fine Root/Remaining Shoot, mass (dry weight)	kgkg <sup>-1</sup>
	40		
	41		

	42		
	43		
	44		
	45		
	46		
	47		
	48		
	49		
	50		
		<b>Regression Coefficients for Needle Number Index</b>	
	51	Previous January Temperature	°F
	52	Previous February Temperature	°F
	53	Previous March Temperature	°F
	54	Previous April	°F
0.04429	55	Previous May	°F
	56	Previous June	°F
	57	Previous July	°F
	58	Previous August	°F
0.017221	59	Previous September	°F
	60	Previous October	°F
-0.03053	61	Previous November	°F
	62	Previous December	°F
	63	Current January Temperature	°F
	64	Current February	°F
0.038246	65	Current March	°F
	66	Current April	°F
	67	Current May	°F
	68	Current June	°F
	69	Current July	°F
	70	Current August	°F
	71	Current September	°F
	72	Current October	°F
	73	Current November	°F
	74	Current December	°F
	75	Previous January Precipitation	Inches
	76	Previous February Precipitation	Inches
0.03391	77	Previous March	Inches
	78	Previous April	Inches
	79	Previous May	Inches
	80	Previous June	Inches
0.033955	81	Previous July	Inches
-0.01793	82	Previous August	Inches
-0.02765	83	Previous September	Inches
	84	Previous October	Inches
-0.0237	85	Previous November	Inches
	86	Previous December	Inches
0.01462	87	Current January Precipitation	Inches
0.021297	88	Current February Precipitation	Inches

0.042747	89	Current March	Inches
	90	Current April	Inches
	91	Current May	Inches
	92	Current June	Inches
	93	Current July	Inches
	94	Current August	Inches
	95	Current September	Inches
	96	Current October	Inches
	97	Current November	Inches
	98	Current December	Inches
-3.72193	99	Regression constant	
	100		

**Table 5.** Filename ‘TRG70.INF’, control parameters (TRG) for TreeRing program

	(A1)Filter temp data (see note 1)
d:\data\model\ Pali1940	(A40) Path for climatic data (A8) File name of climatic data
catalstd.crn	(A12) Indexed Chronology Name
d:\data\model\ cata04Nt	(A40) Path to cell and index dat. (A8) Files CRN - size & thickness
CO2data.car	(A11) File name of CO2 & d13C data

4.0	1	Only simul.(1), with measur(2),+ Index(3), + CO2data (4)
30.0	2	Number of years to write on screen before clearing screen
0.0	3	Force cambium to same state 0-no,1-div,2-enl,3-mat,4-1&2,5-2&3 6-all
1.0	4	Calculate statistics 0-no, 1-yes
1.0	5	Without pause-0, with pause and message-1, with message box-2
1.0	6	Leaf growth STOPS at first limitation-0, CONTINUES after it-1
1.0	7	Graph of cell structure-0, picture of cell structure-1
0.0	8	Cell numbers unchanged-0, estimated numbers normalized to actual-1
1.0	9	Manual control of Input-0, automatic - First climate data year (op.28) -1
1.0	10	Calculate Isotopes-0, don't calculate Isotopes-1
1.0	11	Plots on screen, yes-1, no-0
2.0	12	Output files: 0-only STAT.DAT, 1-P.DAT, 2-all, 3-MClim, 4-only isotope, 5-only #.DAT
0.0	13	Iterate no-0, yes-1, yes and write files and make plots-2
10.0	14	Var-1, rmc-2, rmt-3, grc-4, gc-5, prp-6, upt-7, xrmn-8, xrmx-9, b-10, zini-11
24.0	15	Array sequence number in selected variable type
5.0	16	Control: rw(1), cell#(2), cell sz(3), width(4), 1-4(5), indx(6), all(7), 3, 4, 6(8), 1, 2, 6(9)
2.0	17	Stats:  Av res (0), SD res+ Av res (1), 1-R^2(2),SD+ Av res /SDY(3), Max-Max (4)
20.0	18	Maximum number of iterations allowed before stopping
0.0	19	Krasnoyarsk measurements (0), SilviScan measurements (1)
0.0	20	Use Actual Ring Width for leafmass estimate: No(0), Yes(1)
0.0	21	Iteration averaged with (0,1,2,3 or 4) subsequent parameters moved
6.0	22	Number of iterations on one screen
	23	
	24	
	25	
	26	
	27	
1995	28	Year to end automatic running of model
1940	29	Year to begin reading independent cell measurements
1995	30	Last year of independent cell measurements
	31	
	32	
	33	
	34	
	35	
	36	
	37	

	38		
	39		
	40		
1.0	1		Maximum value of parameter being used for each iteration
0.01	2		Minimum value of parameter being used for each iteration
0.1	3		Step size (DELTA) to begin iteration (in units of parameter)
0.001	4		Step size (TAU) to terminate iteration (in units of parameter)
0.0001	5		Difference in Average Variance to Terminate Iteration

**Table 6.** Description of output parameters from **\*\*\*.P** output files

<b>P(#)</b>	<b>Name</b>	<b>Description</b>
1	Day	Day in year
2	Tem	Daily average temperature ( °C)
3	Pre	Daily precipitation (mm)
4	Sm	Soil moisture (kg m <sup>-3</sup> )
5	PotTr	Potential transpiration (kg H <sub>2</sub> O m <sup>-2</sup> s <sup>-1</sup> )
6	Trans	Transpiration (kg H <sub>2</sub> O m <sup>-2</sup> s <sup>-1</sup> )
7	Rest	Resistance of leaves to diffusion of CO <sub>2</sub> (s m <sup>-1</sup> )
8	Reswb	Resistance of roots to water absorption (s m <sup>-1</sup> )
9	Wab	Water absorption by roots per unit volume of soil (kg m <sup>-3</sup> day <sup>-1</sup> )
10	Ci	CO <sub>2</sub> concentration inside the leaf (mM m <sup>-3</sup> )
11	Phot	Photosynthesis rate (mM CO <sub>2</sub> m <sup>-2</sup> s <sup>-1</sup> )
12	Resp	Respiration (maintenance) rate (mM CO <sub>2</sub> day <sup>-1</sup> )
13	Gleaf	Growth rate of leaves (microns day <sup>-1</sup> )
14	GRcamb	Growth rate of cambial cells (microns day <sup>-1</sup> )
15	GRenla	Growth rate of enlarging cells (microns day <sup>-1</sup> )
16	GRmat	Growth rate of maturing cells (microns day <sup>-1</sup> )
17	Groot	Growth rate of roots (microns day <sup>-1</sup> )
18	SuL	Sucrose in leaves (mM CO <sub>2</sub> )
19	SuS	Sucrose in the stem (mM CO <sub>2</sub> )
20	SuR	Sucrose in roots (mM CO <sub>2</sub> )
21	d13Cps	Carbon isotope composition of photosynthate (‰)
22	d13CstL	Carbon isotope composition of stored starch in leaves (‰)
23	d13CstS	Carbon isotope composition of stored starch in the stem (‰)
24	d13CstR	Carbon isotope composition of stored starch in roots (‰)
25	d13CL	Carbon isotope composition of cellulose in leaves (‰)
26	d13CS	Carbon isotope composition of cellulose in the stem (‰)
27	d13CR	Carbon isotope composition of cellulose in roots (‰)
28	dDps	Hydrogen isotope composition of photosynthate (‰)
29	dDstL	Hydrogen isotope composition of stored starch in leaves (‰)
30	dDstS	Hydrogen isotope composition of stored starch in the stem (‰)
31	dDstR	Hydrogen isotope composition of stored starch in roots (‰)
32	dDCL	Hydrogen isotope composition of cellulose in leaves (‰)
33	dDCS	Hydrogen isotope composition of cellulose in the stem (‰)
34	dDCR	Hydrogen isotope composition of cellulose in roots (‰)
35	d18Ops	Oxygen isotope composition of photosynthate (‰)
36	d18OstL	Oxygen isotope composition of stored starch in leaves (‰)
37	d18OstS	Oxygen isotope composition of stored starch in the stem (‰)
38	d18OstR	Oxygen isotope composition of stored starch in roots (‰)
39	d18OCL	Oxygen isotope composition of cellulose in leaves (‰)
40	d18OCS	Oxygen isotope composition of cellulose in the stem (‰)
41	d18OCR	Oxygen isotope composition of cellulose in stem (‰)
42	Ct	Control on growth
43	Ctm	Control on cell maturation
44	xleaf	Mass of growing leaf tissue (kg)
45	nr	Total number of cells in growth ring
46	nc	Number of cells in the cambial stage
47	ne	Number of cells in the enlargement stage

48	nm	Number of cells in the maturation stage
49	dendgr	Dendrograph trace
50	dgrmin	Dengrograph minimum
51	dgmax	Dendrograph maximum
52	So-Si	Source minus Sink (Photosynthesis minus Respiration + Growth in leaf, stem, root)
53	stemw	Concentration of water in the stem
54	C balan	Carbon balance at end of day
55	LimEnvLf	Limiting environmental factor for leaf growth
56	LimEnvRt	Limiting environmental factor for root growth
57	LimEnvDiv	Limiting environmental factor for cell division
58	LimEnvEnl	Limiting environmental factor for cell enlargement
59	LimEnvMat	Limiting environmental factor for cell maturation
60	d13CCel	Carbon isotope composition of whole cell cellulose (‰)
61	dDvap	Hydrogen isotope composition of atmospheric vapor (‰)
62	dDPrec	Hydrogen isotope composition of precipitation (‰)
63	dDXw	Hydrogen isotope composition of xylem water (‰)
64	dDLw	Hydrogen isotope composition of leaf water (‰)
65	dDCel	Hydrogen isotope composition of cellulose formed during the day (‰)
66	d18Ovap	Oxygen isotope composition of atmospheric vapor (‰)
67	d18OPrec	Oxygen isotope composition of precipitation (‰)
68	d18OXw	Oxygen isotope composition of xylem water (‰)
69	d18OLw	Oxygen isotope composition of leaf water (‰)
70	d18OCel	Oxygen isotope composition of cellulose formed during the day (‰)
71	waterloss	Water loss from leaves per day
72	MaxWLoss	Maximum possible water loss from leaves per day
73	DayLength	Day length (seconds)
74	MxCellSz	Maximum cell size of new years growth cells
75	Contr	Control on growth rate of leaves
76	Contr2	Control to restart growth of leaves
77	d13CstLAr	Carbon isotope composition of stored starch in leaves (‰)
78	d13CstSAr	Carbon isotope composition of stored starch in stem (‰)
79	d13CstRAR	Carbon isotope composition of stored starch in roots (‰)

### III. REFERENCES

- Carey, E.V., DeLucia, E.H., Ball, J.T. 1986. Stem maintenance and construction respiration in *Pinus ponderosa* grown in different concentrations of atmospheric CO<sub>2</sub>. *Tree Phys.* 16:125-130.
- Craig H. and Gordon L.I. 1965. Deuterium and oxygen-18 variations in the ocean and the marine atmosphere. In E. Tongiorgi. *Proceedings of a conference on Stable Isotopes in Oceanographic Studies and Paleotemperatures* 9-130. Spolito, Italy.
- Denne M. P. and Dodd R.S. 1981. The environmental control of xylem differentiation. In: Barnett, J. R. (ed.) *Xylem Cell Development*. Castle House Publ., London, 236-255.
- Farquhar G.D., O'Leary M.H. and Berry J.A. 1982. On the relationship between carbon isotope discrimination and the intercellular carbon dioxide concentration in leaves. *Australian Journal of Plant Physiology* 9:121-137.
- Flanagan L.B. & Ehleringer J.R. 1991. Effects of mild water stress and diurnal changes in temperature and humidity on the stable oxygen and hydrogen isotopic composition of leaf water in *Cornus stolonifera* L. *Plant Physiology* 97:298-305.
- Fondy B.R. and Geiger D.R. 1982. Diurnal pattern of translocation and carbohydrate metabolism in source leaves of *Beta vulgaris*. *Plant Physiology* 70:671-676.
- Freidli, H., Lötscher, H., Oeschger, H., Seigenthaler, U., and Stauffer, B. 1986. Ice core record of the <sup>13</sup>C/<sup>12</sup>C ratio of atmospheric CO<sub>2</sub> in the past two centuries. *Nature* 324, pp. 237-238.
- Fritts H.C., Shashkin A.S. and Downes G.M. 1999. TreeRing 3: A simulation model of conifer ring growth and cell structure. In Wimmer, R. and R. E. Vetter. *Tree Ring Analysis: Biological, Methodological and Environmental Aspects*. CAB International, Wallingford. UK. pp. 3-32.
- Hansen P. 1967. <sup>14</sup>C-studies on apple trees III. The influence of season on storage and mobilization of labeled compounds. *Physiologia Plantarum* 20:1103-1111.
- Hemming D.L., Switsur V.R., Waterhouse J.S. Heaton T.H.E. and Carter A.H.C. 1998. Climate variation and the stable carbon isotope composition of tree ring cellulose: an intercomparison of *Quercus robur*, *Fagus sylvatica* and *Pinus silvestris*. *Tellus* 50B: 25-33.
- Hemming D.L., Jalkanen R. and Leavitt S.W. 2001. Preliminary relationships between climate and the apical extension, needle production and ring width of *Pinus ponderosa* in Arizona, USA. *Palaeobotanist* 50:125-131.
- Keeling, C. D. and Whorf-T. P. 1996. Atmospheric CO<sub>2</sub> records from sites in the SIO air sampling network. In: *Trends: A compendium of data on global change*. Carbon Dioxide Information Analysis Centre, Oak Ridge National Laboratory, Oak Ridge, Tenn., U.S.A.

- Lacointe A., Kajji A., Daudet F-A., Archer P. and Frossard J-S. 1993. Mobilization of carbon reserves in young walnut trees. *Acta Botanica Gallica* 140(4): 435-441.
- Landsberg, J.J. 1986. *Physiological ecology of forest production*. Academic Press, London p89.
- Levin, I., Kromer, B., Schoch-Fischer, H., Bruns, M., Münnich, M., Berdau, D., Vogel, J. C., Münnich, K. O. 1996.  $\Delta^{13}\text{C}$  records from sites in Central Europe. In: *Trends '93: A compendium of data on global change*. (eds Boden, T. A., Kaiser, D. P., Sepanski, R. J. and Stoss, F. W.). ORNL/CDIAC-65. Carbon Dioxide Information Analysis Centre, Oak Ridge National Laboratory, Oak Ridge, Tenn., U.S.A.
- Majoube M. 1971. Fractionnement en oxygène-18 et en deuterium entre l'eau et sa vapeur. *Journal of Chemical Physics* 197:1423-1436.
- Merlivat L. 1978. Molecular diffusivities of  $\text{H}_2^{16}\text{O}$ ,  $\text{HD}^{16}\text{O}$  and  $\text{H}_2^{18}\text{O}$  in gases. *Journal of Chemistry and Physics* 69:2864-2871.
- Monserud R.A. and Marshall J.D. 1999. Allometric crown relations in three northern Idaho conifer species. *Canadian Journal of Forest Research* 29:521-535. Table 5.
- O'Leary, M.H. 1981. Carbon isotope fractionation in plants. *Phytochemistry* 20:553-567.
- Roden J.S., Lin G. and Ehleringer J.R. 2000. A mechanistic model for interpretation of hydrogen and oxygen isotope ratios in tree-ring cellulose. *Geochimica et Cosmochimica Acta* 64(1), 21-35.
- Ryan, M. G., Gower, S. T., Hubbard, R. M., Waring, R. H., Gholz, H. L., Cropper, W. P. Jr., Running, S. W. 1995. Woody tissue maintenance respiration of four conifers in contrasting climates. *Oecologia* 101:133-140.
- Silkin, P.P. 2001. Cell wall masses of conifer tree rings. In: *Tree-rings and People*. Abstract International Conference on the Future of Dendrochronology, Davos 22-26 Sept 2001. WSL, CH-8903 Birmensdorf 2001, p.202-203.
- Taiz L. and Zeiger E. 1991. *Plant Physiology*. Benjamin/Cummings Publishing Co., CA.
- Wardlaw I.F. 1990. The control of carbon partitioning in plants. *New Phytologist* 116:341-381.
- Yakir D. and DeNiro M.J. 1990. Oxygen and hydrogen isotope fractionation during cellulose metabolism in *Lemna gibba* L. *Plant Physiology* 93:325-332.